UNIVERSITY OF BELGRADE

FACULTY OF TECHNOLOGY AND METALLURGY

Ahmed Ali Algellai

Adhesion properties of UV-curing methacrylate - alumina particles composite films for use in dentistry

Doctoral dissertation

Belgrade, 2018

UNIVERZITET U BEOGRADU

TEHNOLOŠKO-METALURŠKI FAKULTET

Ahmed Ali Algellai

Adheziona svojstva fotopolimerizujućih kompozitnih filmova na bazi metakrilata i čestica aluminijum oksida za primenu u stomatologiji

Doktorska disertacija

Beograd, 2018

Acknowledgements

Mentor

Dr Radmila Jančić Heinemann, full professor, University of Belgrade, Faculty of Technology and Metallurgy

Comitte

> Prof. dr Tatjana Volkov Husović, full professor, University of Belgrade, Faculty of Technology and Metallurgy

> Prof. dr Kosovka Obradović Đuričić, full professor, University of Belgrade, Faculty of Stomatology

> Prof. dr Petar Uskoković, full professor, University of Belgrade, Faculty of Technology and Metallurgy

> Prof. Dr Aleksandar Marinković, associate professor, University of Belgrade, Faculty of Technology and Metallurgy

> Dr Dušica Stojanović, senior research associate University of Belgrade, Faculty of Technology and Metallurgy

Candidate:

Ahmed Ali Algellai

> Date of defense: _____

SUMMARY

Adhesion properties of UV-curing methacrylate - alumina particles composite films for use in dentistry

Dental adhesives have an important role in the field of restorative dentistry providing innovative solutions and comfort for the patient. The importance of the quality of the material as well as the adhesion to the substrate are of main importance now days. This thesis deals with composite materials having improved mechanical properties and providing better adhesion to the substrate. The adhesion of the classical composition of photo-polymerizing methacrylate can be improved using the alumina based fillers. It is shown that the substantial improvement is obtained using the chemical modification of fillers composition, and additional improvements are achieved by introduction of the surface modifications on the filler particles. The adhesion is tested using the modified method that uses the hardness measurements to measure adhesion and those results are compared to the wetting angle measurements and to cavitation properties of the composite films. Obtained results suggest that adhesion as well as composite mechanical properties are improved using the selected method.

Key words: composite, adhesion, mechanical properties, dental adhesive, modified surface

Scientific field: technological engineering

Narrow scientific field: materials engineering

REZIME

Adheziona svojstva fotopolimerizujućih kompozitnih filmova na bazi metakrilata i čestica aluminijum oksida za primenu u stomatologiji

Dentalni adhezivi imaju značajnu ulogu u restorativnoj stomatologiji dajući inovativna rešewa I omogućavajući bolji komfor za pacijenta. Značaj kvaliteta materijala, kao I kvliitet adhetije za substrat su posebno značajni u naše vreme. Ova doktorsa disertacija bavi se kompozitnim materijalima koji imaju poboljšana mehanička svojstva I istovremeno boboljšana adhezivna svojstva. Adhezivna svojstva polimera koji se koriste kao adheziv u stomatologiji koji su u stvari fotopolimerizujući metaakrilati mogu se boboljšati dodavawem punilaca na bazi aluminijum-oksida. Pokazano je da se značajna poboljšanja mogu postići hemijskim modifikacijama punilaca, a dodatno se mehanička svojstva I adhezivnost ogu poboljšati površinskom modifikacijom čestica. Adhezija je ispitivana modifikovanom metodom koja je zasnovana na merenju mikrotvrdoće I ovi rezultati upoređeni su sa ostvarenim uglovima kvašewa I svojstvima otpornosti na kavitaciju. Dobijeni rezultati ukazuju da se adhezija kao I mehanička svojstva mogu poboljšati korišćenjem odabranih metoda.

Ključne reči: kompozit, adhezija, mehanička svojstva, dentalni adhetiv, modifikovana površina

Naučna oblast: tehnološko inženjerstvo

Uža naučna oblast: inženjerstvo materijala

1 CONTENTS

FIGURE CAPTIONS

TABLE CAPTIONS

2 INTRODUCTION

The history of humans is usually studied by the archaeology that reveals the habits of the people, including their technical skills and habits, anthropology that studies together with the remains of the material culture the remains of human skeletons. One of the main information about the age and sometimes social position of the person is reflected in the teeth that are studied. Our nutritional habits evolved with the availability of foods and reflected itself in the health of the dental tissue. The people of our days remain impressed that some restorations and reparations were possible in ancient times, but a lot of suffering in everyday life originated from lack of dental treatments.

In our time the dentists are taking care about the population health and their approaches changed with time. Much influence on the dental health comes from the development of technology and materials that are studied in our time. The first important step was done once it was understood that the that eases the process, and introduction of the amalgam in the use in dentistry caries damage could be stopped not only by the extraction of the teeth but also by the extraction of the damaged tissue and restoration of the remaining cavity. The introduction of the turbine machine enabled to generations of people to use their teeth much longer [1]. The toxicity of the mercury was the motivation to search for alternative way to fill the cavity and the answer came from materials science in the form of composites.

The 20th century was the time of polymer development. Almost all synthetic polymer systems were developed in the first part of the last century. The development of different polymer resins was the main advantage that the engineers used in a lot of activities, and dentists took advantage to use materials that are not toxic, last long time, are aesthetically much more advantageous compared to amalgams and enable easy way to fill the cavity and to serve long time without emitting any dangerous materials in the patient body. The new era in aesthetic and comfortable approach began with the introduction of implants in dentistry. The materials for those purposes needed to have a good biocompatibilitiy and remain inert in the body [2]. Titanium was the most accepted metal for those purposes [3].

3 POLYMER BASED MATERIALS

Polymers are molecules having long chains of repeating units that are enabling specific chemical and physical properties. What is interesting in polymers is that their existence is due to the possibility of the carbon atom to bond to another carbon atom and to form those repetitive structures. Polymers are keeping their chemical characteristics independently to the length of the chain; on the contrary some physical characteristic can be influenced by this fact [4]. Polymer structures are found in nature as plants and animals are composed mostly of this sort of materials [5]. Due to their carbon based chemistry, polymers are closer to biological tissue than inorganic materials. The fact of structural similarity can be of interest in targeting some special functionalities in polymers. It is possible to achieve the compatibility of the polymer to the tissue or to some other materials that should be in contact with the biological material.

First man made polymers gained the attention with the discovery of rubber [6] modifications [7] and Bakelite8. In 1930[ties] nylon was discovered and the new era in synthetic polymers begun after the WWII.

Methacrylates were developed as the material having good transparency [9]. Their good compatibility with the human body was noticed early and they find their use as bone cements and in dentistry. The polymerization process of methacrylates is exothermic and can cause tissue damage, so that low amounts should be applied and saline irrigation for cooling may be necessary. This is easily overcome in dentistry as the quantities used are seldom larger than grams. While the polymer is biologically inert, there can be reactions against the monomer and rest-monomers in the polymer [10]. Due to the optical properties (Plexiglass) and inertness in the eye, they are also used as intraocular lenses. The hydrophilic side chains in the hydroxyethyl methacrylate monomer lead to the polymerization to a hydrogel (pHEMA). This has good protein repellant anti-fouling properties and is used for various applications like hemo compatible coatings [11,12] or as lubricant coating on contact lenses [13]. Polymerization of methacrylates can be controlled in different ways and the possibility

to control it using the light is widely used in dentistry to polymerize small quantities rapidly and in a controllable way.

Nowdays the polymers used in dentistry is quite limited. The monomer in the current polymer composite formulas is predominately bisphenol A-glycidyl methacrylate (bisGMA) [14]. However, the hydroxyl groups of bisGMA form intermolecular hydrogen bonds and thus increase the viscosity of the monomer, that is making the workability of this monomer very difficult and use in pure form impossible. Diluent such as triethylene glycidyl dimethacrylate (TEGDMA) is combined with bisGMA in order to make a mixture that enables the use of a monomer as a building agent for dental application . The viscosity of the monomer mixture is reduced, and the workability is achieved, but during polymerization, there is a significant shrinkage due to the linear molecular structure of TEGDMA[15, 16]. The volumetric shrinkage leads to interfacial gaps and residual stresses [17, 18], which affect the long-term mechanical properties of the composites and cause the debonding from the tooth tissue. This phenomenon leads to gaps that leaves ideal space for bacteria attachment, leading to demineralization and tooth decay [19] and limiting the use of the material in time. The introduction of composite materials was aimed to cope with this phenomenon as to diminish shrinkage and to obtain the material that enables improved mechanical propereties.

4 COMPOSITE MATERIALS IN DENTAL ADHESION SYSTEMS

Composite materials are by definition made of at least two different materials that combine together. They preserve their individual properties, but also act together to give an improved combination of characteristics. What is crucial for the functioning of a composite is that the components maintain their individual structure; there is always a surface that is separating two materials [20]. This interphase is a key to composite functioning. All the interactions are passed from one phase to the other by this essential part of the composite. Our body is made of composite structures, our bones, our muscles are functioning as composite materials, and the bone structure consists of a mineral structure interconnected with a protein structure to enable the strengths needed to enable our movement.

The humans have been using different composite materials for a long time; wood is an example of a composite material composed of the lignin that is keeping together the cellulose fibers. Concrete is a composite, but also rocks that are all round us are composites.

Three main classes of materials are metals, ceramics and polymers. Metals have good electrical and heat conductivity, relatively good mechanical properties that range from very stiff metals to some very soft metals like sodium or potassium. Mercury is a liquid metal on room temperature. Ceramics are very stiff, but not as ductile as metals. The main drawback of ceramic materials is their very bad behavior when exposed to tension. On the contrary they can be loaded in compression and behave very well. The electric and heat conductivity of most ceramic materials is bad. Polymers have low elastic modulus, their melting temperatures are low and they are poor in electric and heat conduction. Their ability to be formed is very interesting for material production.
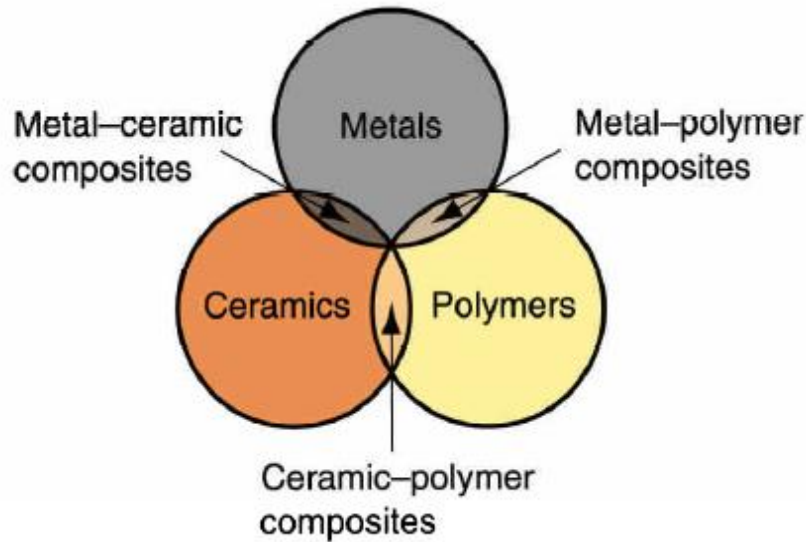
Figure 1 Three different combinations of basic materials that form composites

The composites combine usually the continuous phase that is called the matrix and the discontinuous phase that is called the reinforcement. The aim of the matrix is to give the form to the composite and to enable the establishing of a form of a component, on the other hand the reinforcement is meant to bear the loading. Polymers are usually used as a matrix and ceramic in different form is used as reinforcement to build a composite materials.

If the form and distribution of the phases are considered the composites can be classified following this information. The reinforcement can be in the form of particles distributed in the matrix, forming the particulate composite. If the reinforcement is in the form of continuous fibers than the polymer is distributed round the bundle of fibers and the direction of the fibers is defining the way how the composite is bearing the load. The reinforcement can be in the form of short fibers and the resulting composite is reinforced by the distribution of those fibers in the matrix. The systematization of those composites is given in Figure 2.
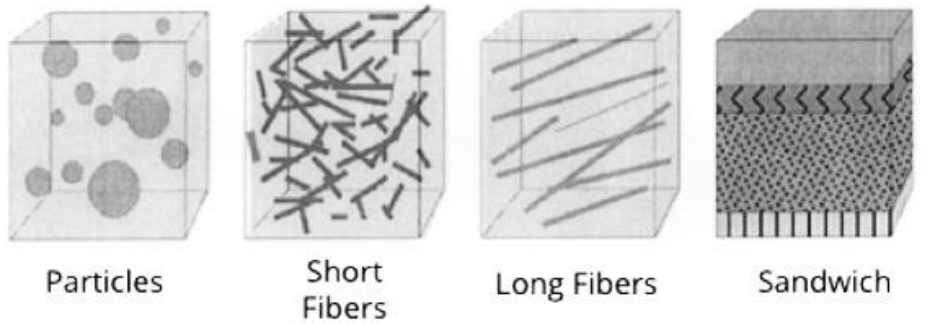
Design and Evaluation of Tribological Coatings, Hogmark, Jacobson, Larsson Wear 246 (2000) 20-33

Figure 2 Types of reinforcements in composite materials [21]

The composite structures incorporate the sandwich structures as well as the structures where two materials function together as layers. The special situation is the one when the material has a layer composed of a polymer or a composite coating on a substrate. There are several phenomena to be studied: the composite itself and the mechanical properties that are considered and the adhesion between the composite and a substrate.

In those situations it is very difficult to obtain good bonding between different materials such as metals and polymers or polymer composites[22]. Chemical bonding between alloys and polymers does not occur spontaneously; composite materials that combine polymers with alloys often suffer from mechanical failure at the interface between them. One example of this challenge is dental devices, which often present catastrophic mechanical failures due to weak bonding between their metallic and polymeric components [23, 24]. These devices include dental prostheses, combining metallic frameworks and wrought wires with acrylic resin; and orthodontic appliances, combining acrylic resin with stainless steel wrought wires.

Another example of metal–acrylic interface found in dental applications is that between wrought wires and acrylic-based dental devices such as dental prostheses and orthodontic appliances [25]. Wrought wires are usually made of stainless steel or cobalt–chromium alloys, which both lack the ability to bind chemically to acrylic resins. Surprisingly, improving the adhesion between wrought wires and acrylic has hardly been investigated.

6

Dental devices combining wrought wires with acrylic such as acrylic removable partial dentures usually cannot be made when not enough volume of PMMA is avail- able to support the wire [26]. By increasing bond strength between stainless steel wrought wire and PMMA through this treatment, more leverage is possible for fabricating acrylic- based dental devices when not enough volume of acrylic is available to support the wire. In this paper we will show a technique to improve the binding between PMMA and alloys used in dental applications based on diazonium chemistry.

5 ADHESIVES, THEIR PROPERTIES AND USE IN DENTISTRY

When considering the adhesion systems the problem is considered as joining together two materials. In dentistry there are two types of adhesion to be considered adhesion to the enamel and adhesion to dentine. On the other hand there can be a list of materials to be joined to the tooth are either resin composite, ceramic or acrylic composite. Dental adhesives should enable adhesion in wet environment that changes the pH every time when the patient is eating. So dental adhesion has several limitations. Types of adhesion to be considered are macro mechanical and micromechanical that are achieved using the glue or cement flowing in the surface irregularities or in blocks of material being glued. Other type of adhesion is achieved when between two surfaces the chemical adhesion takes place joining the two surfaces using the chemical bonding between surfaces. The use of bonding agents such as screws or balts has as a consequence the problem to concentrate stress when there is movement in the mouth. On the other hand the adhesive dispatches this stress to the larger surface and joins the materials so as to act as a unique material.

Polymer materials are very often used as adhesives in industry. Their ability to adhere to different substrates and their possibility to maintain the contact to different materials for a long time made them very often a logical choice to keep two different materials together. In dentistry adhesives are of prime importance in treating the cavity left after the caries removal.

The development and regular use of adhesive materials has begun to revolutionize many aspects of restorative and preventive dentistry. Attitudes towards cavity preparation are altering since, with adhesive materials, it is no longer necessary to prepare the cavity to provide mechanical retention through such features as dovetails, grooves, undercuts, sharp internal angles in order to retain the filling [27]. The new technique has the preservation of large quantities of sound tooth substance that remains in function and therefore enables much more comfort for the patient. Micro leakage a major dental problem, which is probably

responsible for many cases of secondary caries, may be reduced or eliminated. These adhesive are therefore critical for the success of aesthetic materials restorative in modern dentistry [28].

Dental adhesives are resin based materials that make the resin dental substrate interaction achievable. Adhesive systems are composed of monomers with both hydrophilic groups and hydrophobic groups that undergo light curing polymerization to enable the good adhesion to dental tissue. Their composition is chosen so as to wettability to the dental hard tissues, as well as the interaction and co-polymerization with the restorative material [29]. The chemical composition of adhesives also includes curing initiators, inhibitors or stabilizers, solvents and, in some cases, inorganic fillers [30].

The material called hydroxyapatite (HAp) represents a strong structure of the dental tissue enabling intermolecular forces, high-energy surface, besides water and organic material. Dentin is a biological composite of HAp that is surrounded by collagen. Dentin contains water and the hardness is lower than the enamel, with low intermolecular forces and low-energy surfaces. The density of the dental tubular structure is different in different parts of the tooth and the permeation of resin into intertubular dentin will be responsible for most of the bond strength. In deep dentin, dentinal tubules are more in number: the intratubular permeability of resins will be responsible for higher bond strength [31]. With age an increase of dentin thickness and decrease in dentin permeability is observed [32]. Carious dentin suffers structural changes that result in a higher mineralization and a consequently reduced permeability. Unlike dentin, enamel can be dried easily: so bonding process to enamel is different from that of dentin.

The tooth tissues of dentine and enamel compositions can be compared. The enamel consists mainly of hydroxyapatite approximately 95 %, while dentin contains only 50 – 70 % mineral phase, Calcium phosphate ratio is also different in those tissues it is 1.64 in enamel, and 1.56 in dentin. Organic phase is mainly consisting of collagen and in dentin there is only 4-5 % collagen while in dentin there is 20-30 % collagen. Water makes only 1-4 % enamel while the more humid dentin contains 10-20 % water.

Dr. Hagger, a Swiss chemist proposed the use of dental adhesives in 1949. who worked for DeTrey/Amalgamated Dental Company, applied the patent for the first dental adhesive: only dentin was initial substrate for bonding not the enamel. Hagger patented a "Cavity Seal" material to be used in combination with the chemically curing resin "Sevriton", in 1951. This product contained an adhesive called glycerolphosphoric acid dimethacrylate, which was polymerized using a sulfinic acid initiator, later known as "Sevriton Cavity Seal"[28]. This adhesive relies on acidic monomers capable interacting on a molecular level with tooth surfaces in order to form physical/chemical bonds between the restoration and the tooth. Hagger's concept was soon adopted by other investigators and different generations of dental adhesives evolved thereafter, despite the fact it was the first time that bonding to tooth structure became commercially available through the formation of an interface very similar to what is called today the hybrid layer [33]. Mclean and Kramer claimed "Sevriton Cavity Seal", chemically bonded to tooth structure n1952 [34]. This was the first report of changes in dentin promoted by an acidic monomer and may be considered to be the precursor of the hybrid layer concept [34].

In 1954, Buonocore conducted experiments on adhesion to enamel trough acid etching and he focused on altering the enamel surface to obtain a bond with filling material. 85% phosphoric acid was used to alter the enamel surface in 1955 to provide a surface suitable for bonding with resin and also to improve the retention of acrylic resin to pit-and-fissures [35]. Buonocore, Matsui and Gwinnett discussed the effect of phosphoric acid conditioning, which produced "prism-like" tags of resin materials that penetrated enamel surfaces in 1968 [36]. These resin tags were not seen in unconditioned enamel. The effect of phosphoric acid on enamel resulting in increased adhesion was accepted in dentistry but still not widely applied.

The first steps of Minimally Invasive Dentistry were made in 1968 [36]. Enamel conditioning with phosphoric acid results in the formation of micro pores where resin penetrates to form "prism-like" resin tags. The enamel bonding is predominantly micromechanical in nature [37]. While the same concept applied to dentin in 1958 remained problematic, due to the use of strictly hydrophobic resins. As well, the high polymerization shrinkage of acrylic filling

materials gave Buonocore's invention only little impact on Restorative Dentistry at this time. The aim of adding the filler in a composite material beside improvement of mechanical properties is also the reduction of shrinkage due to polymerization. By the mid 1960$_S$, the first commercially available pit-and-fissure sealants and composite resin materials utilizing this new adhesive technology were used clinically. Buonocore by the late 1960s, he also proposed that bonding to dentin [38].

Total-etch concept and the concept of smear layer that blocked adhesion to dentin were being used in the 1970s [39]. By the 1980s, etch-and-rinse adhesive had gained widespread acceptability. Nakabayashi named this new biocomposite by name of hybrid layer in 1982. Moreover, he demonstrated that resin could infiltrate into acid-etched dentin to form a new structure composed of a resin-matrix reinforced by collagen fibrils. At the same time, hybrid layer was considered as the main bonding mechanism of bonding agents. This was best observed by transmission electron microscopy, but was later demonstrated by scanning electron microscopy following argon ion beam etching [40]. In the early 1990s, the introduction of the three-step total-etch adhesive system is new achievement in adhesive dentistry. Once dentin is etched with phosphoric acid and the etchant is rinsed off, hydrophilic primers are used before applying a uniform layer of hydrophobic resin to complete hybridization. However, two-step total-etch adhesive systems and two-step self-etch adhesives were introduced into the market in the late 1990s. Whereas original simple bonding agents evolved to multi-step systems, recent development focuses on simplification of the application procedure in order to abate technique sensitivity and reduce manipulation time.

Smear layer is composed of the tooth tissue from the cavity preparation and this debris. The smear layer is related to the way of cavity preparation and the characteristics of the tissue cut and can be contaminated by saliva and bacteria. The etching is required in order to clear this layer and thus to enable the good bonding to the dentine. There are two ways to overcome this obstacle: to remove the smear layer prior to bonding following etch and rinse procedure, or to use agents that can penetrate beyond the smear layer while incorporating the self-

bonding agents than penetrate beyond the smear layer and propose a self-etch approach. With self-etching systems acidic primers are used to modify or solubilize the smear layer that remains in place but the adhesion can be established [28].
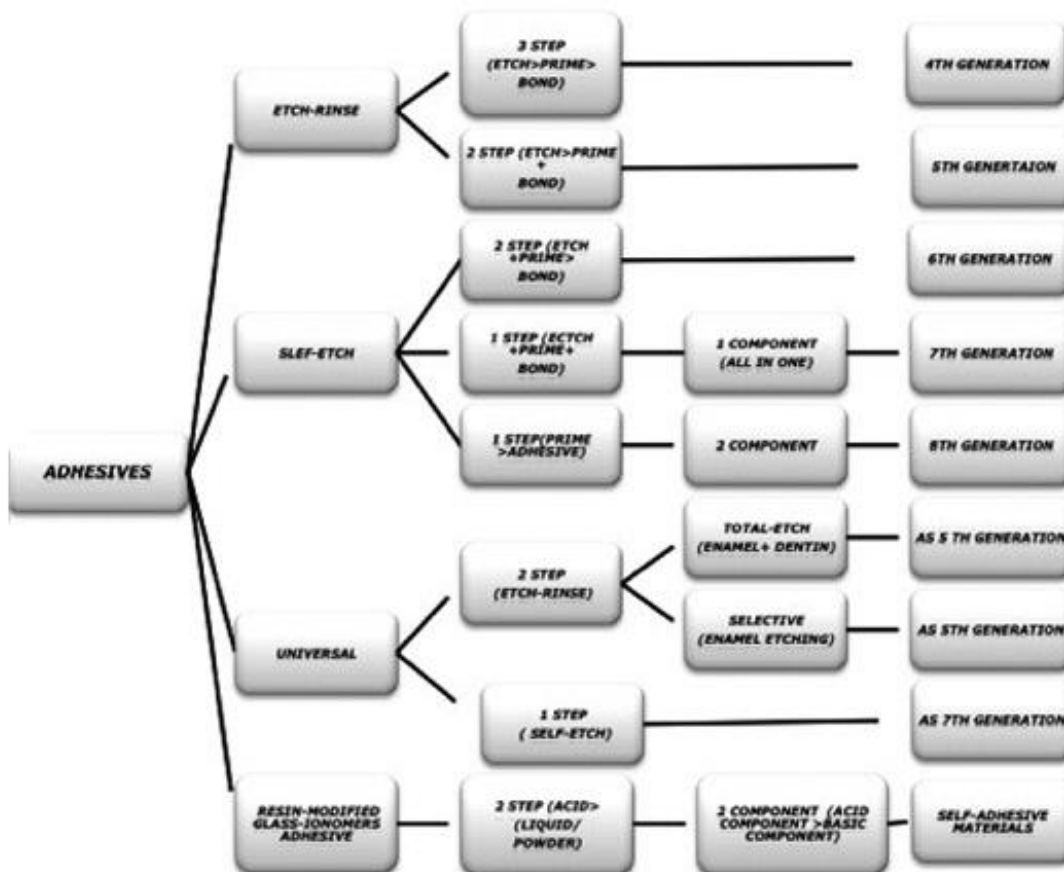
Figure 3 Adhesives by generations [28]

Composite materials are often employed as adhesion improvement systems, mechanical properties improvement, and improvement of adhesion to different substrates dental tissue, metal and ceramic surface.

Many resin adhesive systems and types have been developed to achieve a durable bond to dental tissues. The tooth structure is heterogeneous and this complicates the task of adhesion. There are different strategies to deal with this problem and enable the adhesion to dentine and enamel [41]. Despite the major difference in the manner of etching between etch-and-rinse and self-etch adhesives, the other fundamental steps for adhesion, namely the 'priming' and actual 'bonding' phase, can be either separate or combined. Dental bonding systems are resin blends that possess both hydrophilic and hydrophobic properties by considering the hydrophilic groups enhance the wettability to the dental hard tissues; however, the hydrophobic groups interact and copolymerize with the restorative material and are thus called amphiphilic [42]. Adhesives are compounds containing both hydrophilic and hydrophobic monomers. The major difference between hydrophilic and hydrophobic adhesives is the chemistry of their monomers and solvents. The monomers most used in adhesive system are the hydroxylethyl methacrylate (HEMA) and the Bisphenol glycidyl methacrylate (bis-GMA). The first one, HEMA, is totally miscible in water and serves as an excellent polymerizable wetting agent for dental adhesives. Bis-GMA, instead, is the main monomer used in most dental composites and many adhesives, is much more hydrophobic and will only absorb about 3% water by weight into its structure when polymerized (19). A mixture of the two has intermediate characteristics and serves as a useful adhesive for the tooth.

6 MATERIALS CHARACTERIZATION METHODS

6.1 FTIR

Fourier-transform infrared spectroscopy (FTIR) was used for the characterization of the chemical composition of fillers (nanoparticles based on Al_2O_3, synthesized alumina particles, particles doped with Fe_2O_3 and alumina whiskers) and obtained composite films. Tests were performed using a Nicolet 6700 spectrometer (Thermo Scientific) in the attenuated total reflectance (ATR) mode with a single bounce 45 °F Golden Gate ATR accessory with a diamond crystal, and an electronically cooled DTGS detector. FTIR spectra were obtained at 4 cm^{-1} resolution with ATR correction. The Nicolet 6700 FTIR spectrometer was equipped with OMNIC software and recorded the spectra in the wavelength range from 2.5 μm to 20 μm (i.e., 4000 –500 cm^{-1}).

6.2 HARDNESS MEASUREMENT FOR ADHESION ASSESSMENT

Hardness is the property of a material that enables the study of plastic deformation of a material and enables the relatively easy way to obtain a number of material properties. Methods for hardness measurement incorporate the machine that uses the indenter of defined geometry and composition that is posed on the surface of a material. The indenter is than loaded with a defined force and the resulting action leaves the trace that can be further studied using the optical microscopy. Vickers hardness test is made using the indent in the form of pyramid made of diamond with the possibility to alter the load on the indent. The pyramid has a square base and an angle of 136 degrees between opposite faces subjected to a load of 1 to 100 kgf. The full load is normally applied for 10 to 15 seconds. The two diagonals of the

indentation left in the surface of the material after removal of the load are measured using a microscope and their average calculated. The area of the sloping surface of the indentation is calculated. The Vickers hardness is the quotient obtained by dividing the *F* in kgf load by the square mm area of indentation.

$$HV = \frac{2F\sin\frac{136°}{2}}{d^2} = 1{,}854\frac{F}{d^2}$$

If the loads needed to measure the hardness are lower than those for the standard method then the micro harness testing is done using loads that are lower than 5 N. There is now a trend towards reporting Vickers hardness in SI units (MPa or GPa) particularly in academic papers.
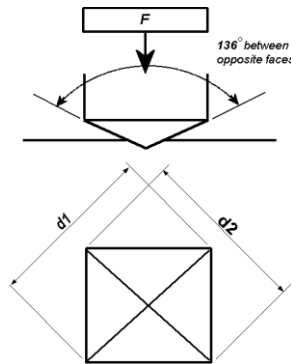
Figure 4 The Vickers hardness measurement basics

The hardness of the samples was measured at micro Vickers machine with different loads (15, 25, 50, 100, 300 and 500 g) for 25 s, whereby for each loading three indents were performed. Images of indentation marks were made by the optical microscope and were used to obtain the diagonal lengths using the Image Pro Plus program for each indent.

The mean diameter of the diagonal's composite hardness is entered as input parameters in the model43 in order to fit the composite hardness relation on the depth indentation by the model shown by the equation:

15

$$H_c = A + B\frac{1}{D} + C\frac{1}{D^{m+1}}$$ (1)

where A, B, C are the fitting parameters, H_c is the composite hardness and m is a parameter called (power index), the values of which are in the range of 1-2 (for soft films on a hard surface m=1.8). The equation used to calculate the film hardness, is given by:

$$H_f = A \pm \sqrt{\frac{[m|B|/(m+1))]^{m+1}}{m|C|}}$$ (2)

For the calculation of the critical reduction of depth b the equation (3) is used

$$\Delta H = \left[\frac{7 \cdot (m+1) \cdot (H_s - H_f)}{m \cdot b}\right] \cdot \frac{t}{d}$$ (3)

The depth of the indentation is supposed to be D/7, and t is the film thickness. Values: H_s, H_c, and d are obtained by direct experimental measurement, H_f is determined by fitting the experimental data for H_c as a function of h / t. Plotting dH = f (t / d) gives the diagram that could be subjected to the linear fit according to the equation (3). The slope of this fit is the value of parameter b that could be considered as the measure of adhesion b. The parameter b, is the ratio of the radius of the plastic zone under indenter and depth of indentation, b = r / h, and it changes depending on the combination of the film and the substrate and is the measure of adhesion.

6.3 METHODS FOR TESTING ADHESION

Adhesion is a phenomenon of importance in a wide range of technologies. This term is used for the fundamental atomic and molecular forces responsible for holding the two phases together [44]. The adhesion test methods for thin coatings are the scratch test, the bending test, the impact test, the cavitation test and the Rockwell indenter test [45], some tests are specially designed to measure adhesion by introducing an additional layer between the adhesive and the substrate [46]. The one of the most popular technique for assessing the

16

adhesion of thin films is microhardness. Hardness has been well established in characterizing metallic materials and ceramics for many years, but only recently it has been widely employed for characterizing polymers (for example: poly(methyl methacrylate) (PMMA) and high density polyethylene (HDPE)) [47] . The adhesion depends on film thickness, substrate hardness, film hardness, indentation depth, etc. [48]. There are several models which can separate the film hardness49 from the composite hardness [50] . Some of the methods are developed for different materials such as metallic coating on a hard substrate [51,52]. Because of its simplicity, [53] the Vickers hardness and the Knoop hardness tests have been used for investigation of hardness of denture teeth or composite resins [54,55] as well as to estimate the mechanical properties of the coatings. The information obtained from the hardness test can separate the properties of the film itself and be used in measuring the adhesion of the film to the substrate by a series of simple measurements and the mathematical model to correlate those results to the adhesion of the film to the substrate.

6.4   CONTACT ANGLE MEASUREMENT

The contact angle is the angle where a liquid–vapor interface meets a solid surface. It is the result of unbalanced surface energies of the three materials meeting in a point. It is the consequence of the wettability of a solid surface by a liquid via the Young equation. A given system of solid, liquid, and vapor at a given temperature and pressure has a unique equilibrium contact angle. However, in practice contact angle hysteresis is observed, ranging from the so-called advancing (maximal) contact angle to the receding (minimal) contact angle. The equilibrium contact is within those values, and can be calculated from them. The equilibrium contact angle reflects the relative strength of the liquid, solid, and vapor molecular interaction.

The shape of a liquid–vapor interface is determined by the Young-Laplace equation where the contact angle is a boundary condition via the Young equation. The theoretical description of contact arises from the consideration of a thermodynamic equilibrium among three phases liquid phase (L), the solid phase (S), and the gas phase (G). If the solid–vapor interfacial

energy is denoted by γ_{SG}, the solid–liquid interfacial energy by γ_{SL}, and the liquid–vapor interfacial energy by γ_{LG} , then the equilibrium contact angle θ_C is determined from these quantities by the Young equation:

$$\gamma_{SG} - \gamma_{SL} - \gamma_{LG}cos\theta_C = 0$$

The contact angle can also be related to the work of adhesion in the Young Dupre equation:

$$\gamma(1 + cos\theta_C) = \Delta W_{SLW}$$

where ΔW_{SLV} is the solid – liquid adhesion energy per unit area when in the medium V. The lower the angle of θ_C is the better the adhesion between the solid and the liquid is.
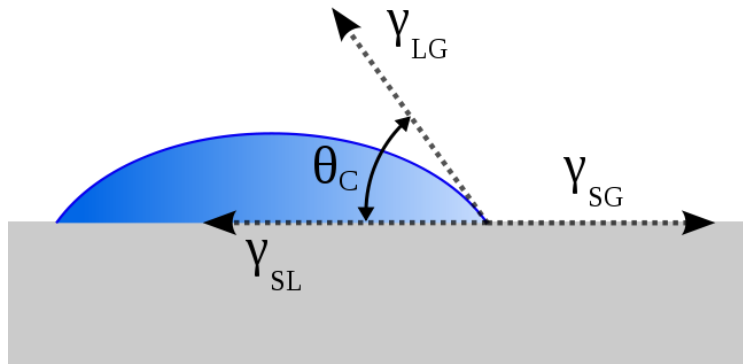
Figure 5 Schematic of a liquid drop showing the quantities in the Young equation.

In studies of the composite preparation the contact angle has the very important role. Contact angle can be to evaluate the compatibility of different surfaces [56] and therefore it can be used to evaluate the adhesion [57] between the surfaces in contact [58,59]. The unbalanced forces on the interface cause it to contract to a minimum surface area value and the work required to increase the area of a surface is called surface tension [60]. The chemical composition and established interactions in contact materials determines the relative contribution of each component to surface tension [61]. Wetting angle is strongly influenced

by the surface tension and determines if the adhesive will fulfil the surface defects which are the precondition to effective adhesion.

The contact angle can be measured using microscopy technique that enables a precise imaging of the contact established between the drop of a liquid and a substrate. The digitalized image can then be used to determine the angle using image analysis techniques where this is one of the basic features.

Adhesion of the composite film on the metal surface was monitored *via* wetting angle determination. Drop of the composite mixtures was placed on a metal substrate and polymerized using the UV lamp. The same procedure was done with the matrix material. The images of the samples were taken with an optical microscope (Smart 5MP Pro) and the contact angles of the composite to the metal surface were determined using the image analysis software.

6.5 CAVITATION

Cavitation is the process where the surface of the material is exposed to the rapid fluid jet. Cavitation happens when the pressure in a liquid suddenly drops. The drop in pressure is caused by pushing a liquid quicker than it can react, leaving behind an area of low pressure often as a bubble of gas.The surface destruction depends on the properties of the material and if the surface is coated than the cavitation can be used to evaluate the quality of the adhesion between the base material and the coating. G. L. García et al. investigated cavitation resistance of epoxy-based multilayer coating systems [56]. C. Creton et al. investigated the effect of the adhesive film thickness on the cavitation process. They used blends of a symmetric styrene-isoprene-styrene triblock copolymer [57] in their studies of cavitation behavior of polymer materials. The wear characteristics of zirconia filled PMMA were investigated in order to obtain information about the possibility of this filler to improve wear resistance [62].

Cavitation erosion test was performed using the ultrasonic vibration method (with stationary sample) applying water flow (5-10 ml/s), according to ASTM G32 standard. The same conditions developed for testing of metallic materials were applied in previous work, for different types of materials (ceramics [63], composites [64], coatings [65]), castables and refractories.
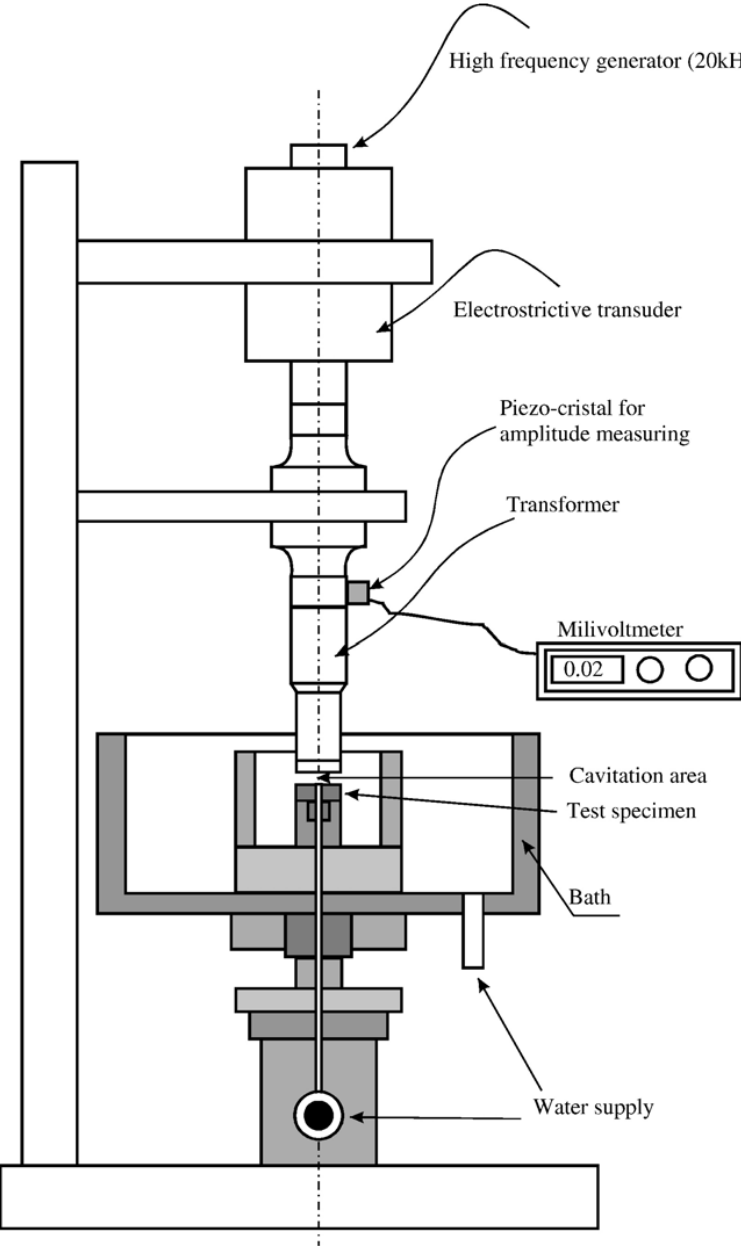
Figure 6 Schematic overview of cavitation test set up [66].

The cavitation test is performed in water tank where the sample surfaces are exposed to high power ultrasound. This test attacks the surface at many spots and can lead to destruction of film material. Cavitation erosion testing was accomplished utilizing the

recommended standard values:

- Frequency of vibration: 20 ± 0.2 kHz

- Amplitude of vibrations at the top of the transformer: $50\pm2\mu$m0

- Gap between the test specimen and the transformer: 0.5 mm

- Temperature of water in the bath: 25 ± 1 °C

- Ordinary water flow: from 5 to 10 ml/s

Cavitation can be monitored using the mass loss measurements and by measuring corresponding surface degradation by means of image analysis in determined time intervals of cavitation. Comparison of those methods gives a lot of information about the process and thus can be interpreted in more detail. The films cold be observed in regular time intervals, and observation noted in order to obtain data for further analysis. Specimens should be dried and their mass measured and then photographed using the scanner in order to minimize the influence of light conditions. Image analysis of the photographs of the sample surfaces was done using image analysis software [67,68] that allowed to measure levels of the surface damage during cavitation erosion [69]. At first the contrast of the image was enlarged in order to be able to separate destructed to not destructed parts of the film. The difference on the grey scale produced by this method was used in order to separate the destructed and not destructed parts of the surface. Then the obtained results are presented in the form of binary objects in the image.

6.6 IMAGING TECHNIQUES

Computerized imaging techniques applied to the field of material science has a great contribution in providing the information about microstructures and failures. The computer is an indispensable tool for managing information and recording programs from various scanning devices that are retrieved and read out by a central computer bank. This technology has provided computer graphics and image analysis, and changed testing procedures, and given materials scientists a more accurate analysis tool that saves considerable time.

6.6.1 Scanning electron microscopy (SEM)

The Scanning Electron Microscope (SEM) is used for observation of specimen surfaces. When the specimen is irradiated with a fine electron beam (called an electron probe), secondary electrons are emitted from the specimen surface. Topography of the surface can be observed by two-dimensional scanning of the electron probe over the surface and acquisition of an image from the detected secondary electrons.

The SEM requires an electron optical system to produce an electron probe, a specimen stage to place the specimen, a secondary-electron detector to collect secondary electrons, an image display unit, and an operation system to perform various operations (Figure 7). The electron optical system consists of an electron gun, a condenser lens and an objective lens to produce an electron probe, a scanning coil to scan the electron probe, and other components.

The electron optical system (inside of the microscope column) and a space surrounding the specimen are kept at vacuum.
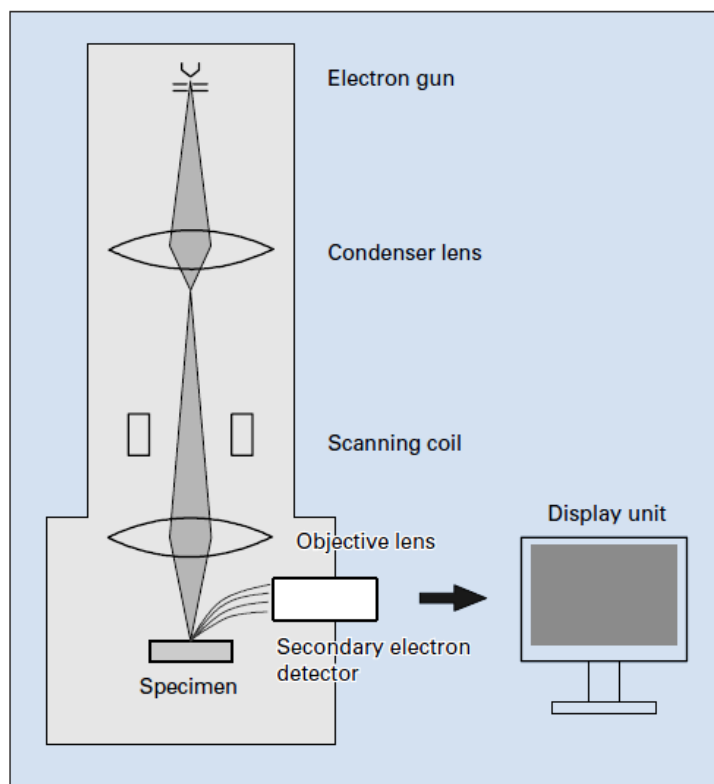
Figure 7 Basic construction of a SEM.70

The morphologies of the composite with different fillers were examined using a field emission scanning electron microscope (FESEM), MIRA3 TESCAN, operated at 3 kV.

6.6.2   Optical microscopy

The past decade has witnessed an enormous growth in the application of optical microscopy for micron and submicron level investigations in a wide variety of disciplines [71]. A typical upright compound reflected light (illustrated in Figure 8) microscope also equipped for transmitted light has two eyepiece viewing tubes and often a trinocular tube head for mounting a conventional or digital/video camera system. Built-in light sources range from 20 and 100 watt tungsten-halide bulbs to higher energy mercury vapor or xenon lamps that are used in fluorescence microscopy. Light passes from the lamp house through a vertical illuminator interposed above the nosepiece but below the underside of the viewing tube head.

The specimen's top surface is upright on the stage facing the objective, which has been rotated into the microscope's optical axis.

In reflected light microscopy, absorption and diffraction of the incident light rays by the specimen often lead to readily discernible variations in the image, from black through various shades of gray, or color if the specimen is colored.
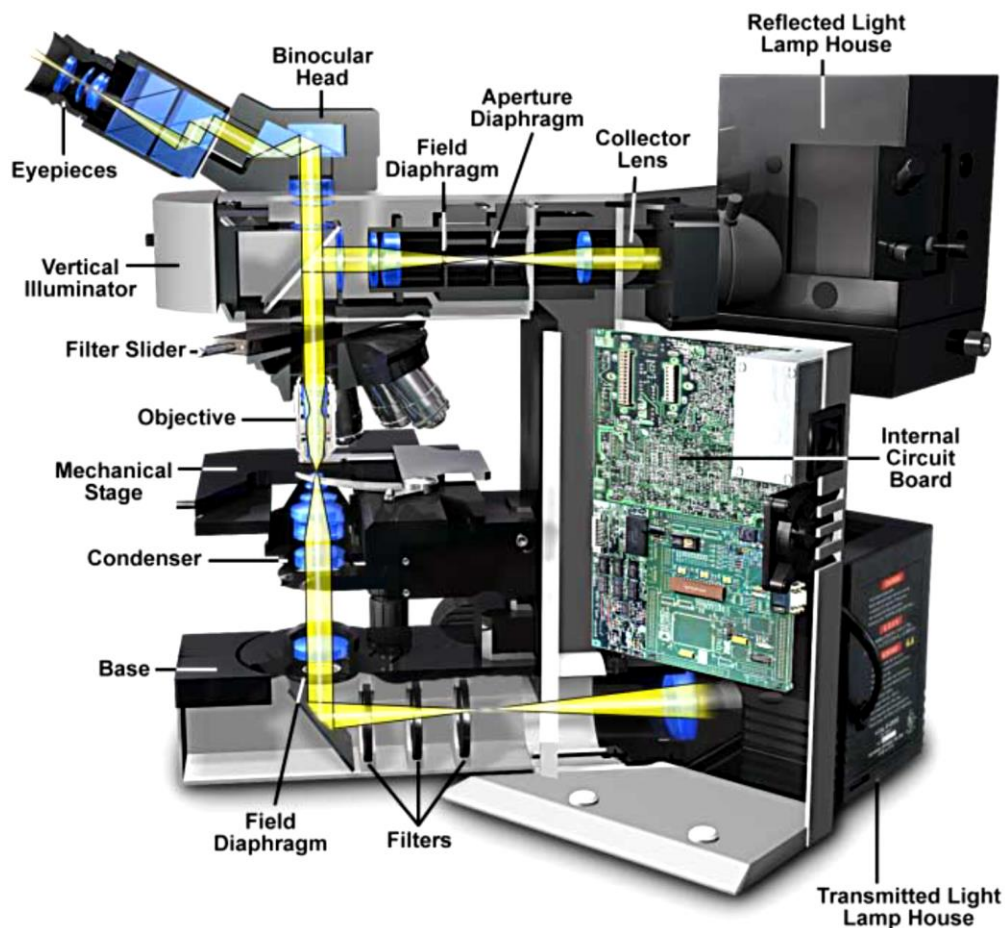
Figure 8 Components of a modern microscope configured for both transmitted and reflected light. This cutaway diagram reveals the ray traces and lens components of the microscope's optical trains. Also illustrated are the basic microscope components including two lamp houses, the microscope built-in vertical and base illuminators, condenser, objectives, eyepieces, filters, sliders, collector lenses, field, and aperture diaphragms.

6.6.3 Image analysis

Image-Pro Plus is the ultimate image analysis software package for fluorescence imaging, quality assurance, materials imaging, and various other scientific, medical, and industrial applications. The most powerful member of the Image-Pro software family, Image-Pro Plus includes extensive enhancement and measurement tools and allows you to write application-specific macros and plug-ins.

Measuring

Fast, accurate, and repeatable results with measurement options including:

• Tracking tools allow you to automatically follow objects in a sequence image and measure distance traveled,

• Snap feature allows you to automatically save measurements into images for documentation,

• Calibration Wizard helps you to calibrate an active image and create reference and system calibrations,

• Length, area, perimeter, and angle tools,

• Best-fit line, arc, and circle metrology tools,

• Automatic count and size tools include over 50 measurement options,

• Watershed, auto-split, and cluster analysis tools to resolve clustered objects,

• Caliper tool for edge detection and measurement.

Analyzing

Test, compare, and analyze your data for maximum results.

• Visualize image data with scattergrams, histograms, line profiles, and surface plots,

• Produce gray scale, color, and 3D representations of co-localization with automatic measurements,

• Analyze RGB, HSI, HSV, or YIQ content of color images,

• Add, subtract, or mask images with Boolean or arithmetic functions,

• Export data to statistical and spreadsheet packages.

EXPERIMENTAL PART

7 GOAL OF RESEARCH

The aim of this work was to evaluate the adhesion of the composite film to the metal substrate. The first step is to prepare several composites having different alumina based fillers and to choose the one having the best performance among the produced composites. The adhesion properties are to be studied using the microhardness method and the results compared to the contact angle measurements and resistance to cavitation. The adhesion of composite films based on Bis-GMA/TEGDMA monomers reinforced with alumina based fillers on brass surface is examined. Three different methods are used:

(I) Determination of the hardness of the film and the quantitative assessment of adhesive strength C-G model according to the Chen Gao model;

(II) Wetting angle between the composite and the substrate determination; and

(III) The cavitation testing.

The method based on microhardness measurement is adapted from the studies for stiff films on metal substrates so the results needed to be proved by other methods that would test the adhesion of the composite film on the metal substrate. The contact angle measurement was the obvious choice as it provides data about the surface tension balance between the adhesive and the substrate that is related to compatibility of two layers. Cavitation studies are used to study the resistance of the material to wear and friction with a fluid that causes destruction of the film. This method directly acts to the breaking of the adhesion between the substrate and the film and therefore was suitable to be used to prove the results from the microhardness measurements. The methods used in this study were proven be consistent to attain the information about adhesion, and to enable the use of the microhardness measurements for accurate measurement of the adhesion as the simple and efficient method.

8 MATERIALS AND SAMPLE PREPARATION

8.1 MATERIALS

8.1.1 Substrate

As a metal substrate the brass thin sheet having hardness 1.483 GPa was used. This material was used as a representative metallic material and it was possible to obtain the sheet of defined structure and good surface finishing.

8.1.2 Polymer matrix

The composite films were made on the surface of this metal in order to determinate the adhesion of the composite film to metallic surfaces. The film is cured under UV lamp, three minutes for each sample.

8.1.3 Preparation of particles

Other two different fillers were synthesized via the sol gel technique: $Al_2Cl(OH)_5 \times 2.5\ H_2O$ and demineralized water formed the sol that was transformed in the gel. The gel was heat treated at 900 °C in order to obtain the suitable crystal structure for reinforcement of the matrix. The same procedure was followed to produce Fe_2O_3 doped particles, $Al_2Cl(OH)_5 \times 2.5\ H_2O$ and $FeCl_3 \cdot 6H_2O$ formed the sol. The amount of Fe_2O_3 precursor was adjusted so as to obtain 10 wt. % Fe_2O_3 in the final composition of particles.

The alumina particles were synthesized via the sol gel technique: $Al_2Cl(OH)_5 \cdot 2.5\ H_2O$, $FeCl_3 \cdot 6H_2O$ and demineralized water as a solvent. Demineralized water and aluminum chlorohydrate were mixed using a magnetic stirrer until complete dissolution and then 1.5

wt. % of $FeCl_3 \cdot 6H_2O$ was added under continued stirring. The mixture solution was then poured into a Petri dish and allowed to gel. The resulting mixture was ground in a mortar and the powder was calcined at 900 °C for two hours. The amount of Fe_2O_3 precursor was adjusted so as to obtain 10 wt. % Fe_2O_3 in the final particle composition. The gel was heat-treated at 900 °C in order to obtain the appropriate crystal structure of the reinforcement[72]. The particle size of alumina doped with iron oxide was previously determined by particle size analyzer. The most commonly used metrics when describing particle size distributions are d-values d(0.1), d(0.5) and d(0.9)) which are the diameters from the intercepts for 10%, 50% and 90% of the cumulative number of particles. The diameters of such obtained particles are: d(0.1) = 0.412 µm, d(0.5) = 0.608 µm, d(0.9) = 1.208 µm (in other words, the values in brackets represents the percentage of analyzed particles in the range of 0.0-1.0 having diameter up to the specified value) 73. According to the obtained results, calcined Al_2O_3 Fe powder was of submicron sizes.

8.1.4   Particles surface modification

8.1.4.1   Synthesis of methyl ester from linseed oil fatty acid (biodiesel – BD)

In a four-necked glass reactor of 2 l, equipped with a reflux condenser, mechanical stirrer, thermometer and a dropping funnel, 929 g (3.3 mol) of linseed oil, dissolved in 85 ml of methanol, was added. Next, a potassium hydroxide solution in methanol (0.12 mol of KOH in 102 ml of methanol) was added drop wise. The reaction mixture was then heated to 58–62 °C for 3 hours, and left to cool down. The bottom layer, i.e. mainly raw glycerin, was separated, and the upper layer was treated with active charcoal and filtered through diatomaceous earth. After drying with sodium sulfate, the obtained linseed oil methyl ester (biodiesel, BD) was purified by vacuum distillation under nitrogen. Characteristics of the obtained mixture, termed BD were: the acid value (AV) 5 mg KOH/g; ester content 97 %; iodine value 152 [73].

Alumina particles (1 g) were dispersed in toluene (75 ml) using a mechanical stirrer in under reflux under the flow of nitrogen. When the boiling point of toluene was reached (110.6 ºC), 1 g of silane coupling agent (VTMOEO/MEMO/APTMS) was added and the reaction was kept for 22 h. After the completion of the reaction time, the particles were filtrated and washed with hexane in order to remove unreacted silane. The particles were dried at 40 ^{0}C in an oven for 12 h and then used for preparation of composites [14]. The Al_2O_3 Fe particles modified with VTMOEO, MEMO and APTMS were denoted as Al_2O_3 Fe – VT, Al_2O_3 Fe – ME, and Al_2O_3 Fe – AM, respectively.

8.1.4.2   Second step of alumina modification with BD

The modified alumina particles with terminal amino groups (Al_2O_3 Fe – AM), from the first step of alumina modification, were dispersed in 50 ml THF and 1.56 g of methyl ester of linseed oil fatty acids in a three-necked glass reactor, equipped with a magnetic stirrer, thermometer, reflux condenser and a calcium chloride protection tube. The reaction was carried out for 12 h at 25 °C, whereupon the mixture was kept at 60 °C for 2 hours. The obtained particles were filtered under vacuum, followed by dispersion in THF and filtration (two times), washed with absolute ethanol and dried at 40 °C for 12 h. The particles obtained in this modification step were denoted as Al_2O_3 Fe – BD.

8.1.5   Composite preparation

The composite matrix components were Bis-GMA (Bisphenol A glycidylmethacrylat) 49.5 %, TEGDMA (triethylene glycol dimethacrylate) 49.5 %, CQ (Camphorquinone) 0.2 % and 4EDMAB (ethyl-4-dimethylaminobenzoate), 0.8 % all supplied by Sigma - Aldrich. Commercial alumina fillers were used as received from Sigma - Aldrich. The spherical

aluminum oxide nanoparticles were declared to have a diameter of less than 50 nm and were obtained from Sigma - Aldrich. The alumina whiskers were also commercially available from Sigma - Aldrich, and they were characterized by diameters of 2–4 nm and lengths of 200–400 nm.

The composites using ferrous oxide modified alumina fillers were made with 1 wt. %, 3 wt. %, 5 wt. % and 10 wt. % of fillers. The decision about the type and amounts of fillers added was based on the previous knowledge based on the experiments using electrospun fibrous fillers [74,75] and on commercially available alumina particles and whiskers [76]. The particles produced for this purpose were larger in diameter and no surface modification was applied so the higher amount of filler was tested. The specimens were in form of disks having the 5 mm diameter and 2 mm thickness that enabled the hardness determination.

9 ADHESION AND PHYSICAL MECHANICAL PROPERTIES OF FERROUS OXIDE DOPED ALUMINA FILLERS AND ACRYLATE MATRIX

9.1 RESULTS OF MICROSTRUCTURAL STUDY

The microstructures of composites with 5 wt. % of different fillers were examined using the field emission electron microscope. The material of the matrix is rather homogeneous especially in the composite with the synthesized alumina particles doped with iron. Most of the agglomerates are dispersed but some remain visible in the structure, Figure 9.
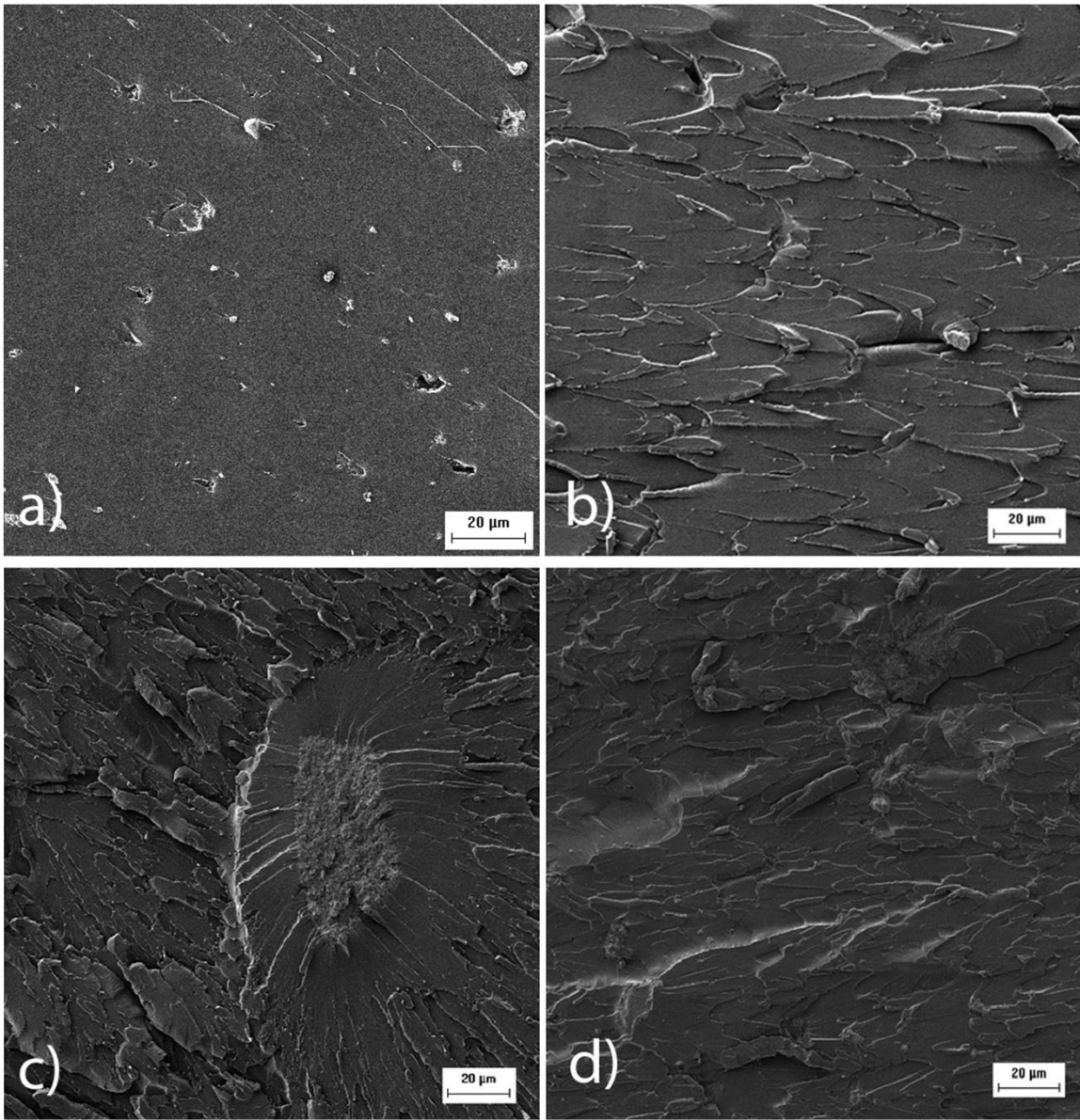
Figure 9 FESEM images of the specimen structure having 5 wt % of the different fillers a) the alumina particles doped with iron oxide, b) synthesized alumina particles, c) nano alumina particles and d) whiskers.

9.2 FTIR CHARACTERIZATION OF FILLERS AND COMPOSITE FILMS

The FTIR spectra of fillers are shown in Figure 10. The characteristic peaks of whiskers and alumina particles doped with iron observed at $3000 - 3500$ cm^{-1} can be assigned to O-H groups. The peak at 1637 cm^{-1} corresponds to the bending of the H–O–H bonds. Cluster of Al^{3+} and O^{2-} ions on the surface of alumina is attributed to the peaks at 1078 cm^{-1}.The peaks at 744 and 628 cm^{-1}are attributed to the Al – O bonds [77], that are supposed to arise from a pseudo-boehmite structure. Frequencies are reported at 630 cm^{-1} for the Al–O stretching mode and at 736 cm^{-1} for the torsional mode [78]. The FTIR spectrum of alumina fillers shows the main differences at the bands centered at $\approx$600 and $\approx$800 cm^{-1}, assigned to the vibrations of the Al–O bonds in tetrahedral and octahedral environments, respectively, which suggested that the synthesized alumina fillers had a γ crystalline structure. Increased O-H vibration for commercial alumina nanoparticles and whiskers than observed in synthesized alumina particles and alumina doped with iron oxide, indicate the higher amount of water absorbed at the particles surface. This could be explained by the fact that synthesized particles are examined and used just after the calcination process.

Figure 10 Comparison of FTIR spectra for fillers used in composites preparation: a) nano alumina particles, b) synthesized alumina particles, c) the alumina particles doped with iron oxide, d) whiskers.

The FTIR spectra of composites with the same amount of different fillers and composite films with alumina based particles are shown in Figure 11.
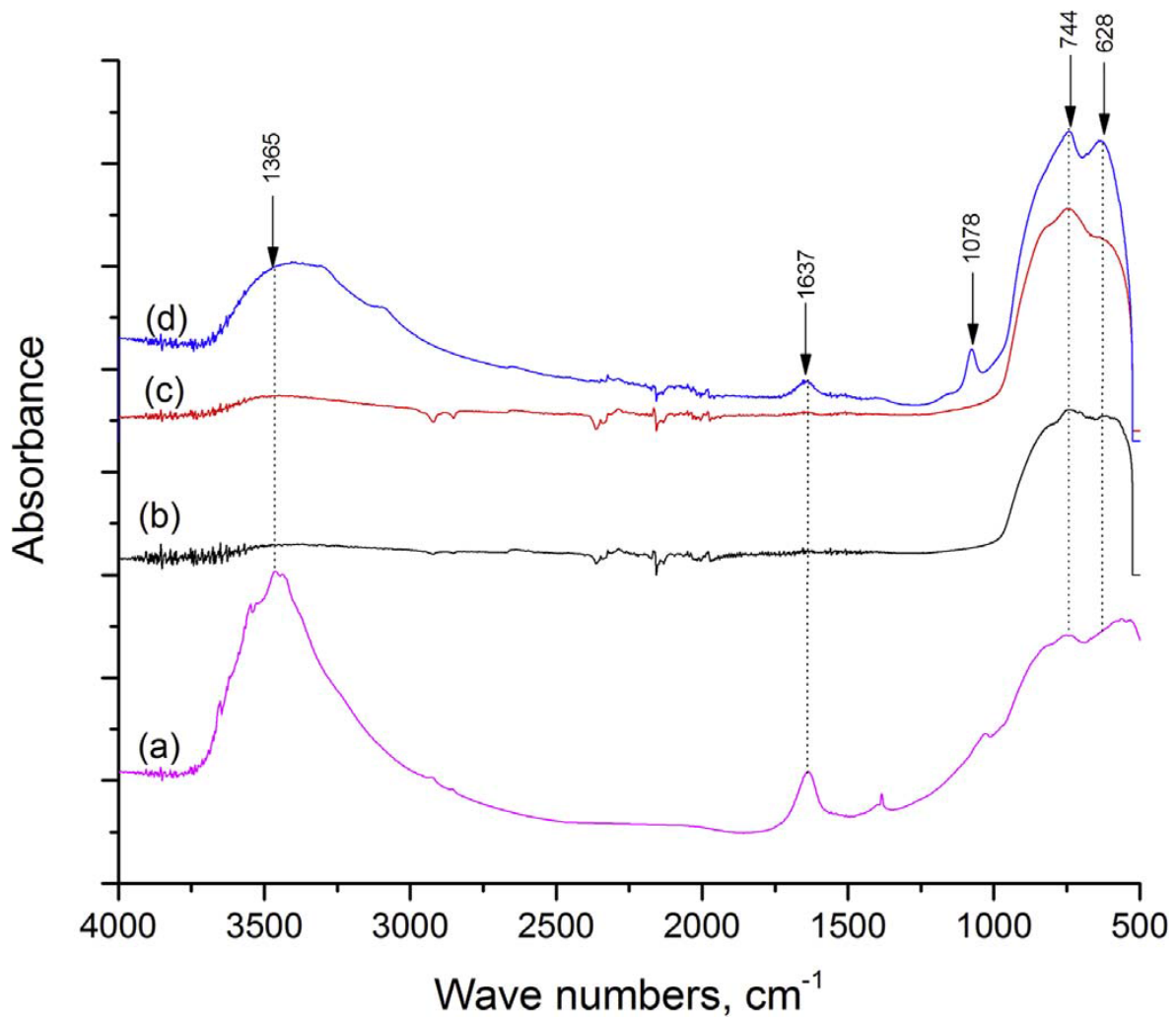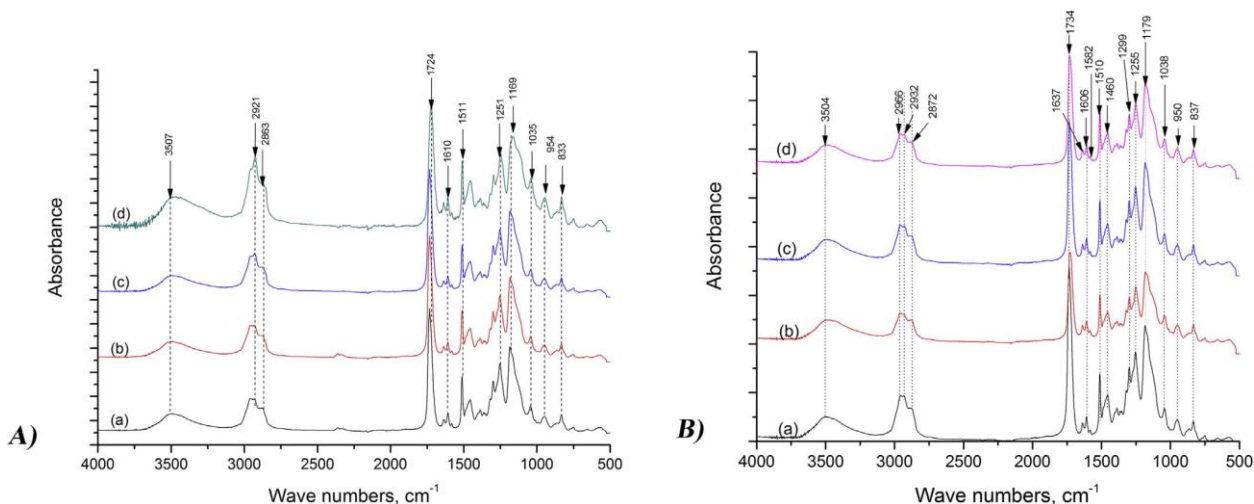
Figure 11 a) FTIR spectra of composite having 5 wt % of different fillers a) synthesized alumina particles doped with iron oxide, b) synthesized alumina particles, c) whiskers, d) nano alumina particles and B) FTIR spectra of composite films with different extent of synthesized alumina particles doped with iron oxide: a) matrix polymer, b) 3 wt % of particles, c) 5 wt % of particles and d) 10 wt % of particles.

The characteristic peaks at 3500 cm^{-1} can be assigned to O-H stretching vibration. The peaks at 2966, 2932 and 2872 are attributed to the aliphatic C–H stretch of the matrix [79]. The peak positioned at 1734 cm^{-1} correspond to the carbonyl C=O bond of Bis-GMA and TEGDMA. The double carbon bonds are registered using the absorbance peak intensities for the C=C bonds at 1637 cm^{-1} (peak corresponding to the aliphatic chains) and C=C bonds at 1606 cm^{-1} and 1582 cm^{-1} (peak corresponding to the aromatic chains) [80]. In plane bending of N-H stretching is observed at 1510 cm^{-1}. The absorption peaks at 1460 cm^{-1} are present due to skeletal vibrations of aromatic rings. Out-of-plane bending vibration modes of aromatic C–H bonds are observed at 1299, 1255, 1179, 1038 cm^{-1}. The absorption peaks observed below 1000 cm^{-1} illustrated in-plane-bending vibration modes of C–H bonds [77]. It can be observed that the incorporation of the particles didn't cause any structural changes of the matrix except of lowering the intensity of peaks due to the higher amount of particles

used while the intensity of O-H vibration remained due the contribution of surface hydroxyl groups of the particles.

9.3   MICROHARDNESS OF COMPOSITES

Microhardness of prepared composites increased with increasing the amount of fillers. The composite without fillers has microhardness of 0.1881 GPa and the composite with the particles based on aluminum oxide doped with iron oxide have the best resistance to indentation and the best hardness increase. Microhardness of composites with addition of 10 wt. % of filler increases from 66 % to 85 % compared to the pure matrix material depending on the type of filler. The microhardness results are presented in Figure 12.
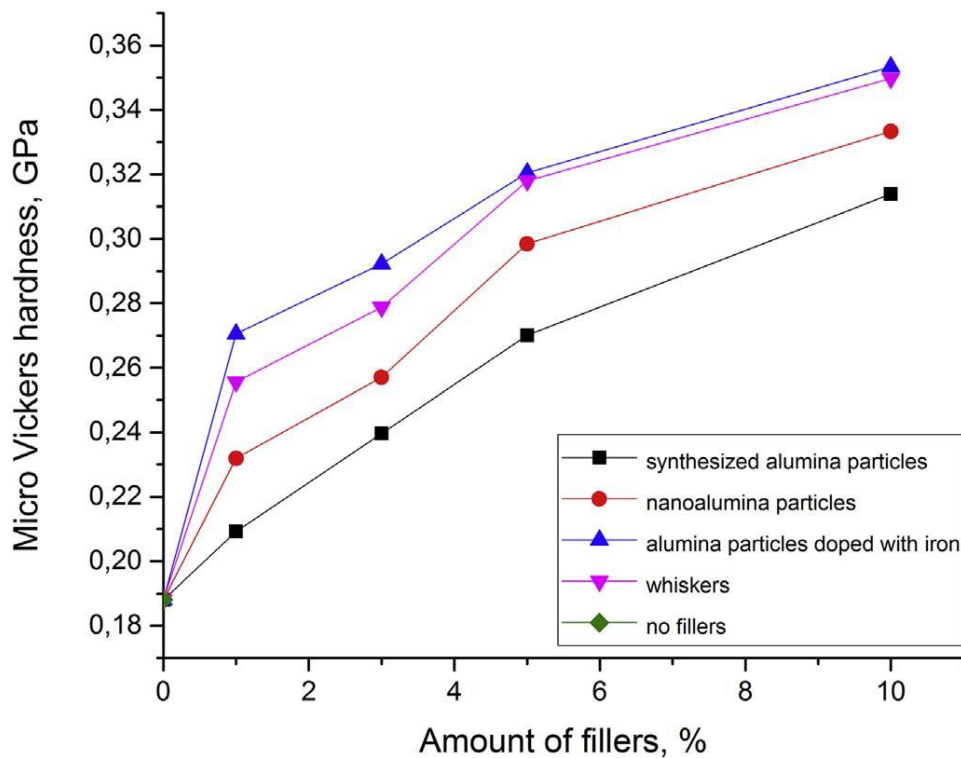
Figure 12 Micro hardness changes regarding the amount of fillers

Alumina - ferrous oxide doped particles added to PMMA produced the composite material exhibiting the best microhardness value so this filler was used for investigation of the adhesion between the composite film and metallic surfaces. Improved hardness of obtained composite is usually accompanied with the increase of the resistance to wear, cutting, and scratching that increase the applicability of composites. Micrographs of micro Vickers indentation for composite with 3 wt. % of different fillers are shown in Figure 13.
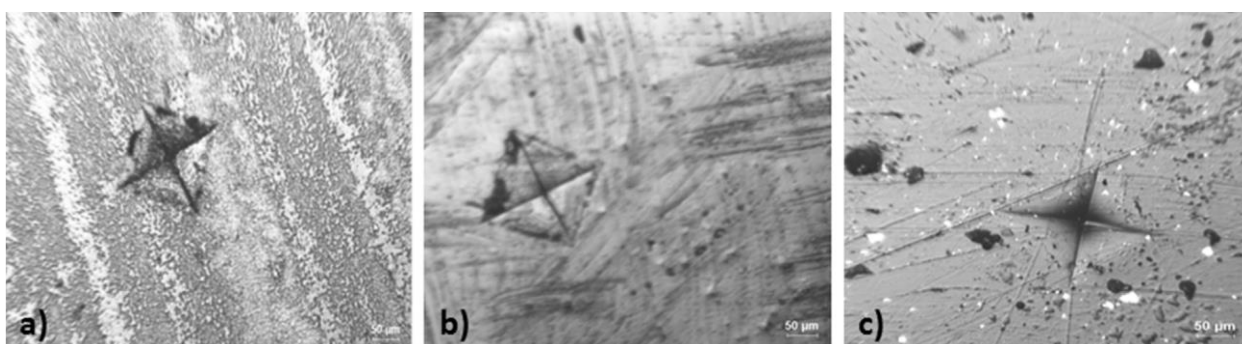
Figure 13 Micrograph of micro Vickers indentation for composite: a) with 3 wt. % of synthesized alumina particles, b) with 3 wt. % of nanoalumina particles and c) with 3 wt. % of whiskers.

Micrographs of micro Vickers indentation for composite films with different amount of the alumina particles doped with iron oxide are shown in Figure 14.
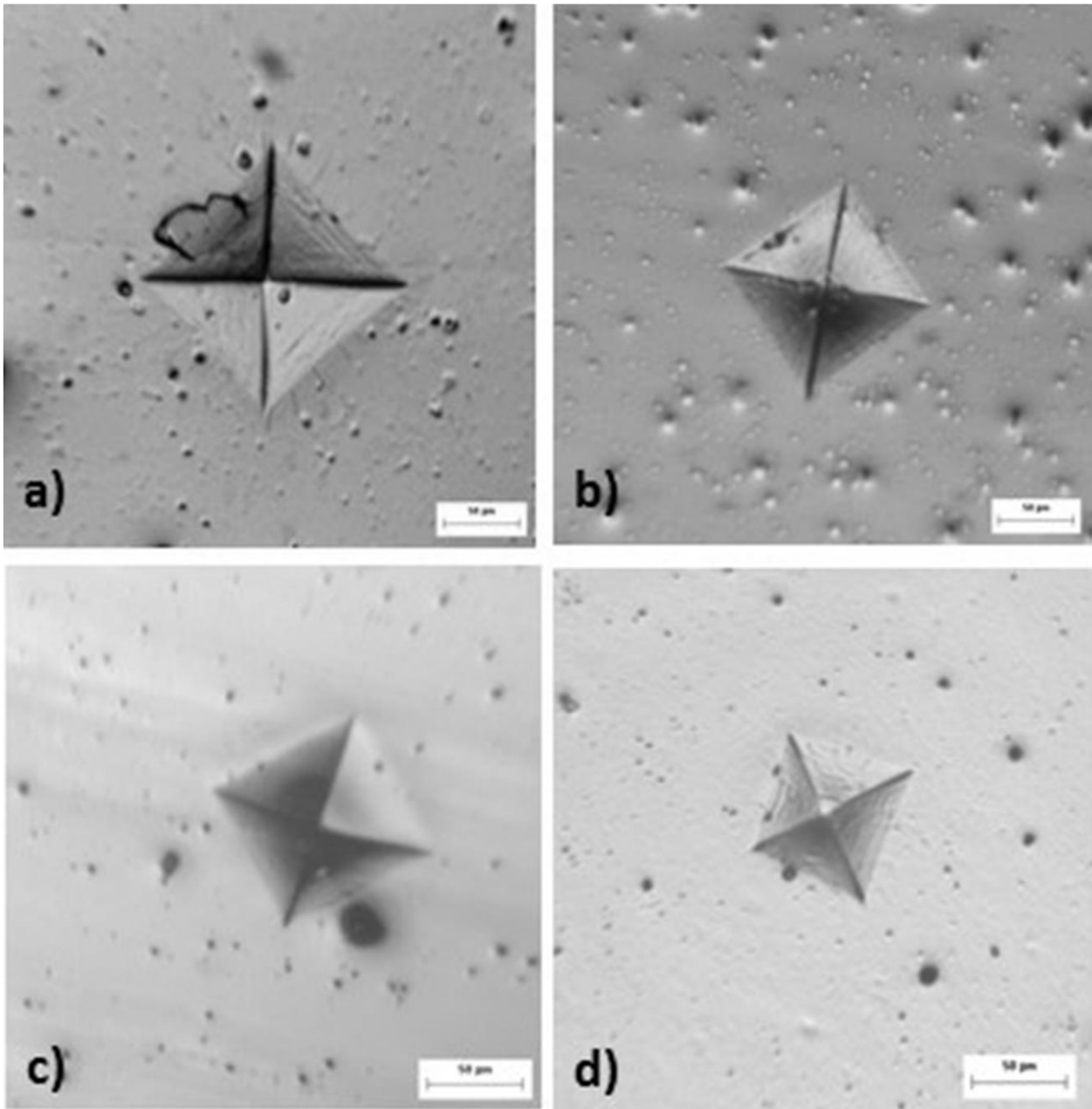
Figure 14 Micrograph of micro Vickers indentation for composite films: a) without particles, b) with 3 wt. % of particles, c) with 5 wt. % of particles and d) with 10 wt. % of particles.

As it can be seen the indent is getting smaller in size as the amount of fillers increases resulting in the corresponding hardness increase.

The set of measurements is made with different loads on microhardness testing machine. The obtained results are used to calculate the adhesion of the film to the substrate as described earlier. Adhesion increases linearly with the share of particles in a composite film, as shown in Figure 15. The parameter, b, is the ratio of the radius of the plastic zone under indenter and depth of indentation, $b = r / h$, and it changes depending on the combination of the film and the substrate and adhesion between them.
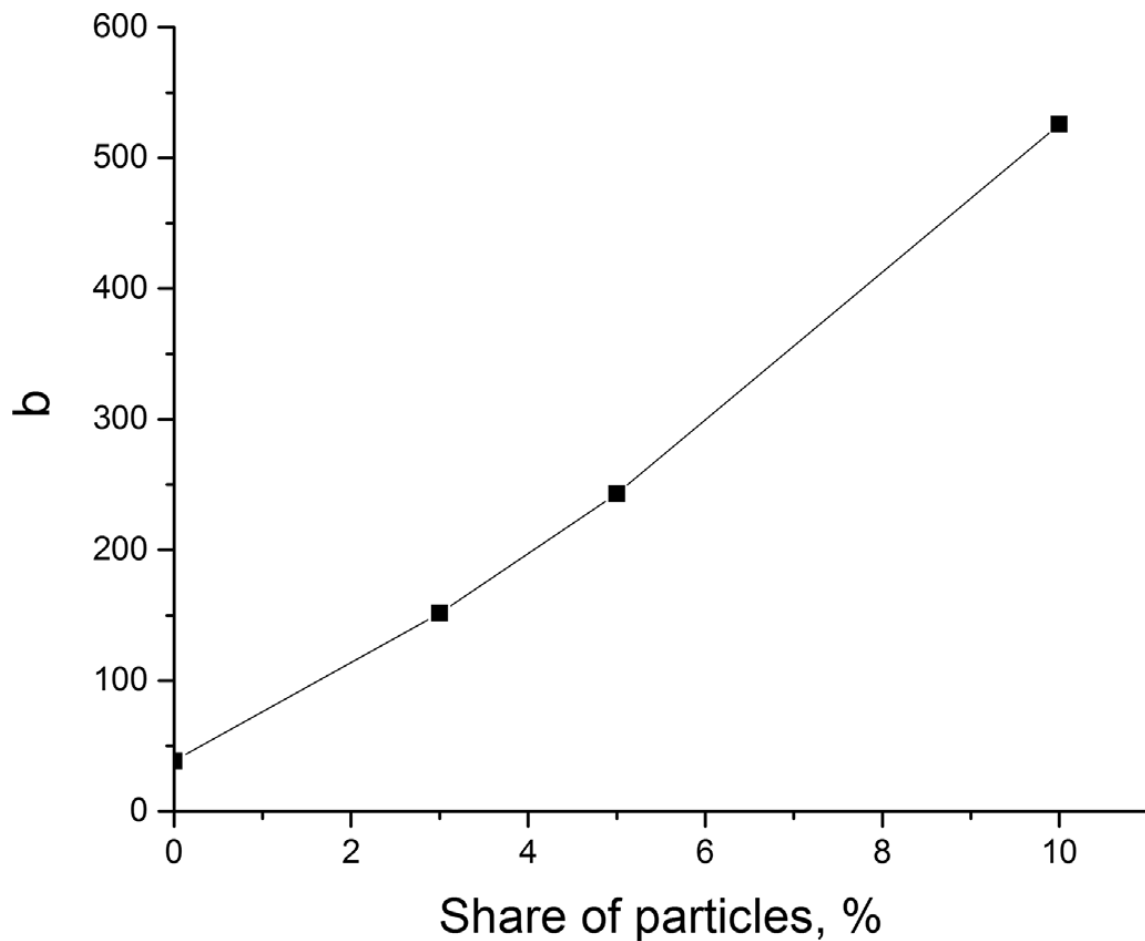
Figure 15 The dependence of the adhesion strength parameter b of the particles share.

9.4 WETTING ANGLE

The images of wetting angles for samples of pure polymer and the prepared composite films are shown in Figure 16.
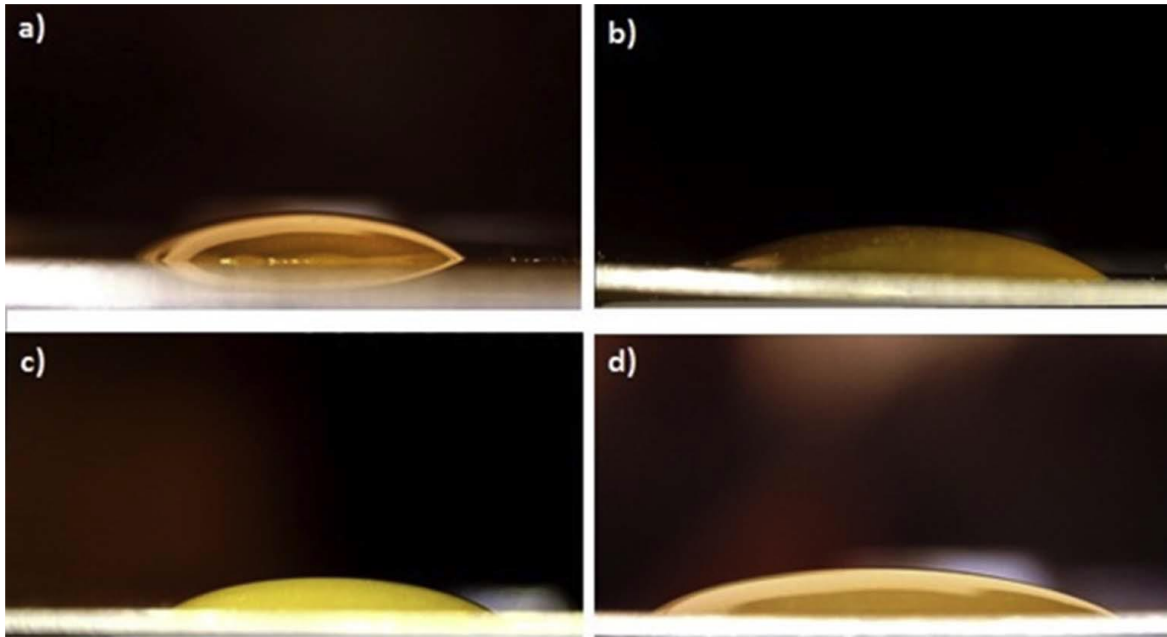
Figure 16 Wetting angle for samples: a) samples without particles, b) with 3 wt. % of particles, c) with 5 wt. % of particles and d) with 10 wt. % of particles.

The contact angles of composite mixture with particles based on aluminum oxide doped with iron, decreased with increasing the share of particles in the composite. Decrease of contact angle for different composite films is obvious in Figure 16. The measured contact angles are presented in function of particles share in the composite. Low contact angle enable good wetting and then the adhesive flows into the valleys and crevices on the metal surface. Higher contact angle results in poor wetting when the adhesive bridges over the valleys and results in a reduction of the actual contact area between the adhesive and the adherent, resulting in a lower overall joint strength.

The electrostatic mechanism is a plausible explanation for polymer-metal adhesion joints [81]. The presence of surface charge imbalance means that the adhesive and metal surface

will exhibit attractive forces. Introducing the higher amount of polar alumina particles contributes to higher surface charge imbalance, which yields static electricity generated by touching two differing surfaces together (composite adhesive/metal) causing stronger adhesive bonding. The increase of attractive forces between the metal substrate and the adhesive with increasing the share of the particles is reflected by the decrease of contact angle Figure 17.
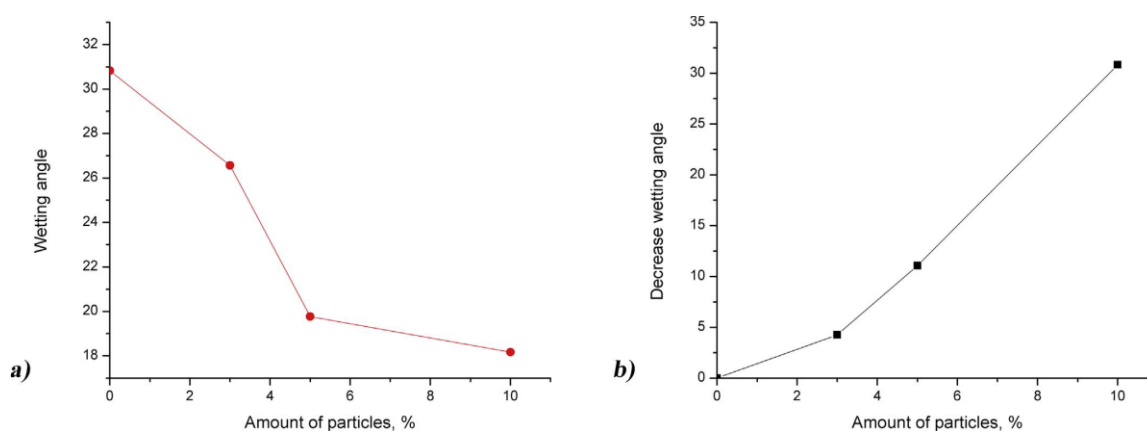
Figure 17 Decrease of wetting angle dependence on the amount of particles in the composite film on the brass substrate.

The structure of inter between the composite film and the substrate was shown in Figure 18. The composite that was studied has 3 wt. % of ferrous oxide doped alumina particles and it can be seen that the contact between the film and the substrate is very good, the wetting of the surface enables good contact between two different phases and enables good bonding. The inner surface of composite film indicated the inverse microstructure of metal surface which was the result of lower surface tension that allowed fulfillment of valleys and crevices.
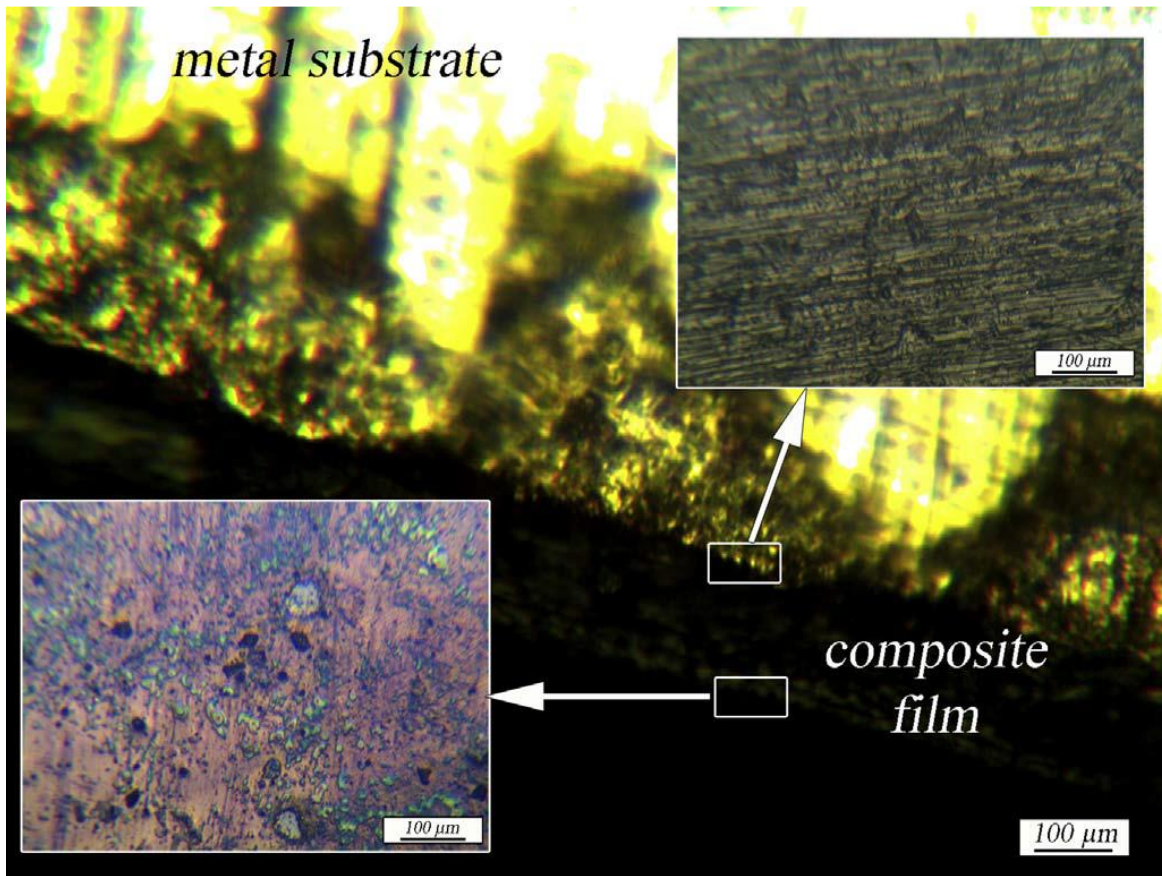
Figure 18 Cross-section of the contact surface of the composite film and substrate

9.5   RESULTS OF CAVITATION EROSION TESTING

The images showing surface defects after 1 min of cavitation for samples made of pure polymer and composite films with 3 wt. %, 5 wt. % and 10 wt. % of particles are shown in Figure 19.
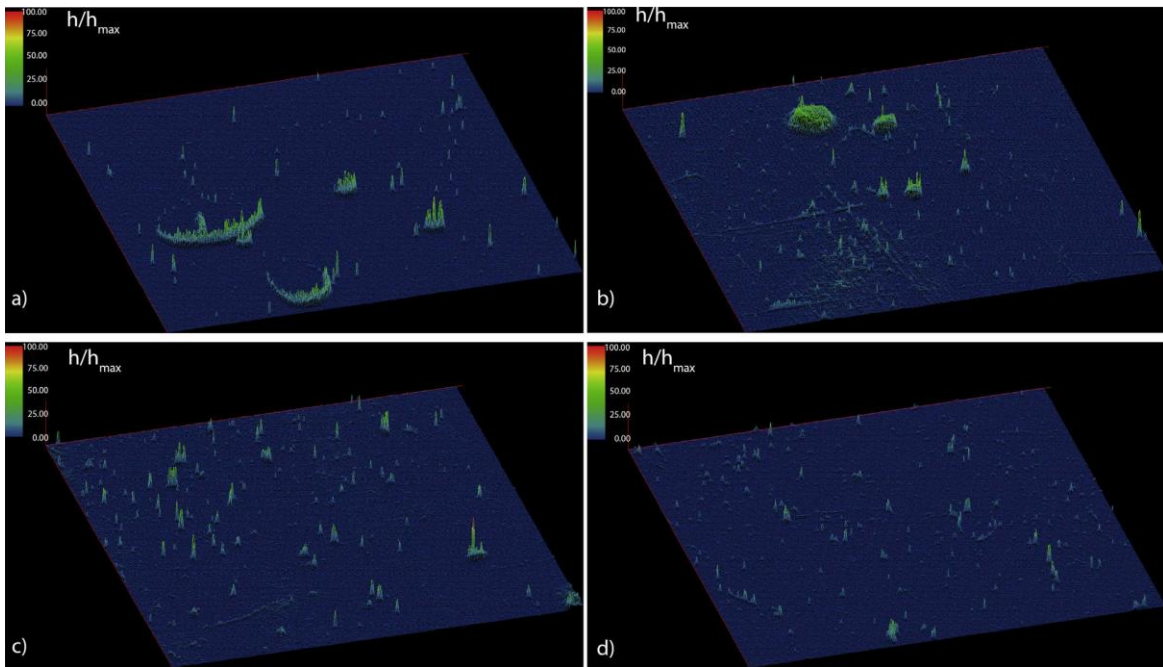
Figure 19 Surface plot images after 1 min of cavitation for samples: a) without particles, b) with 3 wt. % of particles, c) with 5 wt. % of particles and d) with 10 wt. % of particles. The height of the z axis corresponds to the depth of erosion on the surface.
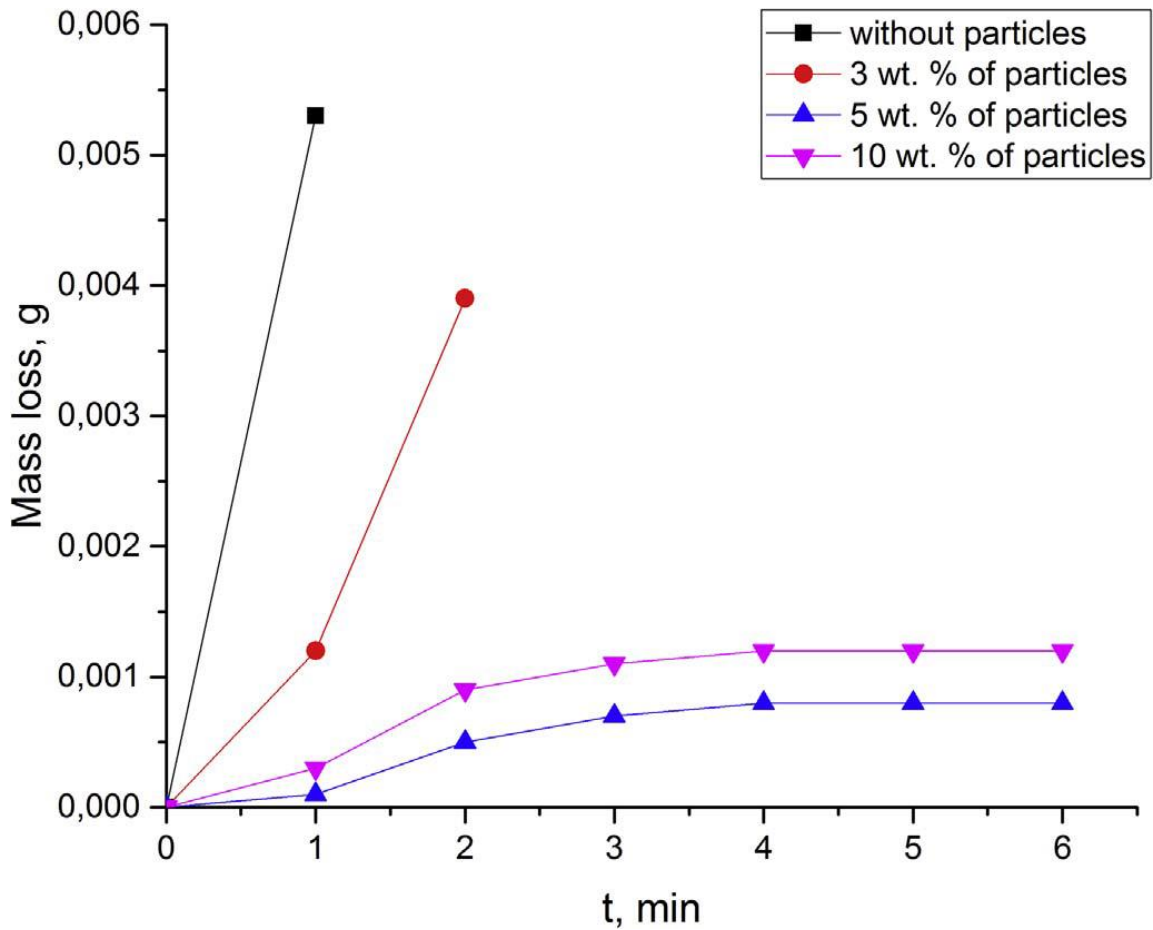
Figure 20 Mass loss during cavitation resistance testing.

Mass loss of samples of pure polymer and samples with 3 wt. % of the particles is significantly higher than the samples with 5 wt. % and 10 wt. % of the particles. The specimen without particles was completely destroyed after 1 min of exposure to cavitation and exhibited significant mass loss. The specimen having 3 wt. % of particles lasts 2 min under the same conditions before being destroyed. Samples with 5 wt. % and 10 wt. % of the particles exhibit no sensible difference in the cavitation rate. The better behavior of the film having 5 wt. % of particles could be explained by the dispersion of particles in the polymer. The share of 10 wt. % of particles is probably too high and the dispersion not as good as in the sample having 5 wt. % of particles. On the other hand, the surface of the destructed area behaves as in Figure 21.
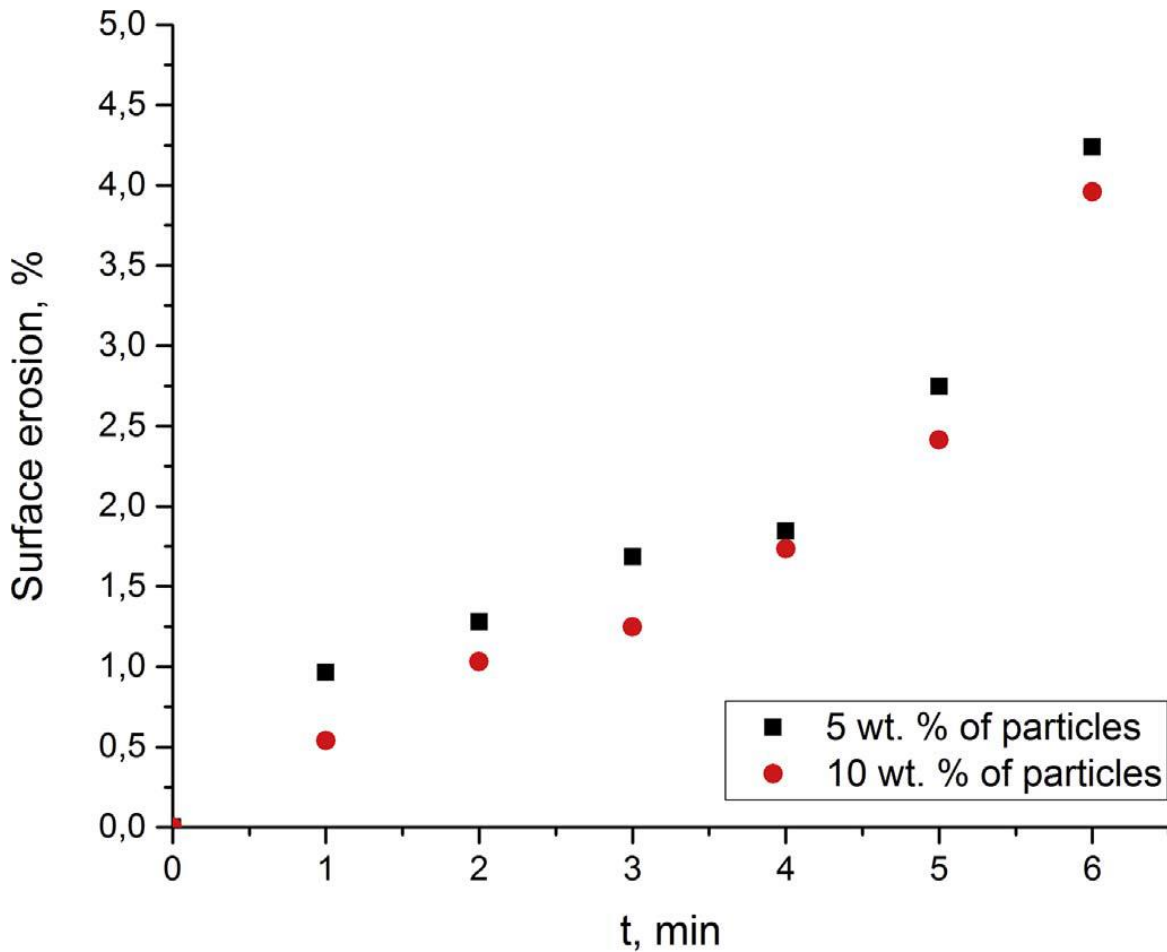
Figure 21 The progress of the surface destruction under cavitation erosion.

The specimens having 5 wt. % and 10 wt. % of particles behave in the same mass loss and their surface destruction is significantly slower than the destruction of the pure polymer film or the film having 3 wt. % of particles. This could be explained by better adhesion of the film on the metal surface. The rate of surface destruction progress as the slope of the curve showing the surface destruction progress can be considered as a measure of adhesion quality. Another way to show the cavitation rate could be the mass loss per unit time, Figure 22. This parameter could be considered as inversely proportional to the adhesion intensity. According

to those observations the adhesion is better when the share of the particles is larger as confirmed by other two methods.
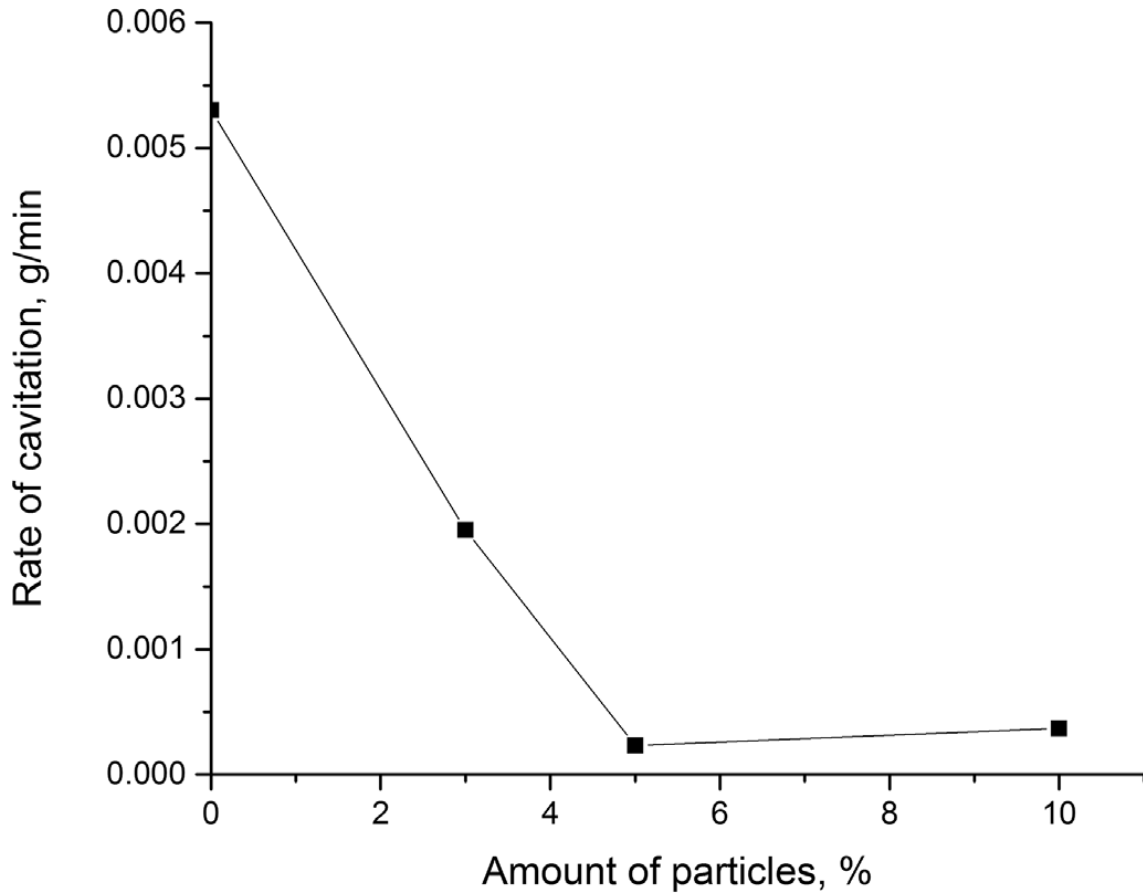
Figure 22 The dependence of the rate of cavitation vs. share of particles in composite films.

In order to identify the relation between the adhesion parameters, the correlation statistics was performed and presented in

Table 1. According to the correlation coefficients, it can be noticed that the increase of particle amount is followed by the increase of adhesion parameter (*b*), decrease of wetting angle and thus by reducing of cavitation rate. Negative values of correlation coefficients represent the reverse linear dependence.

The specimen having 10 wt.% of the filler did not exhibit better resistance to cavitation compared to the one having 5 wt.% of the filler. As the filler amount increases it is possible that some agglomerates form in the specimen and cause the local failure of the material under cavitation. It was observed that the film having 10 wt.% of the filler exhibit some points where the cavitation was more advanced and those observations could be explained by the formation of agglomerates in the composite. The agglomerate formation can be avoided using the functionalization of particles and compatibilization to the polymer, but this process is rather time consuming and expensive.

Table 1 Correlation coefficients obtained for adhesion related parameters

	Amount of particles, wt. %	*Adhesion parameter*	*Decrease of wetting angle, °*	*Wetting angle, °*	*Cavitation rate, g/min*
Amount of particles, wt. %	1				
Adhesion parameter	0,9950	1			
Decrease of wetting angle, °	0,9806	0,9948	1		
Wetting angle, °	-0,9217	-0,8880	-0,8586	1	
Cavitation rate, g/min	-0,8288	-0,7691	-0,7085	0,9411	1

10 THE COMPOSITE HAVING FUNCTIONALIZED ALUMINA PARTICLES AS FILLERS

10.1 MORPHOLOGICAL CHARACTERISTICS OF MODIFIED PARTICLES

Morphologies of Al_2O_3 Fe with four different surface modifications (MEMO, VTMOEO, APTMS and BD) are shown in Figure 23 together with the measured particle diameter distribution.
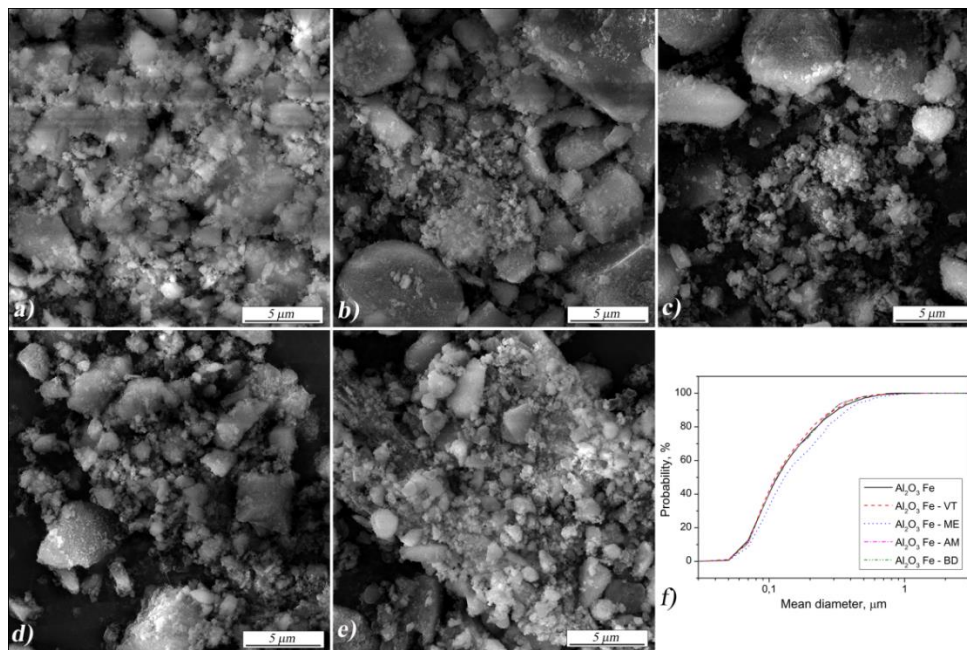
Figure 23 The FE-SEM micrographs of: a) Al_2O_3 Fe, b) Al_2O_3 Fe $-$ VT, c) Al_2O_3 Fe $-$ ME, d) Al_2O_3 Fe $-$ AM, e) Al_2O_3 Fe $-$ BD and f) cumulative particle diameter of analyzed particles.

Statistical data of morphological properties of Al_2O_3 Fe with and without surface modification are given in Table 2.

Table 2 Statistical data of morphological particle properties (values in parentheses represent standard deviation)

Statistical data	Area, μm^2	D_{max}, μm	D_{min}, μm	D_{mean}, μm	Roundness	Fractal dimension	No. of objects analyzed
Al_2O_3 Fe	0.026 (0.055)	0.294 (0.270)	0.075 (0.054)	0.171 (0.123)	5.502 (5.220)	1.153 (0.074)	1197
Al_2O_3 Fe – VT	0.023 (0.050)	0.280 (0.267)	0.074 (0.055)	0.165 (0.124)	5.266 (4.339)	1.146 (0.075)	756
Al_2O_3 Fe – ME	0.037 (0.077)	0.343 (0.337)	0.094 (0.074)	0.200 (0.155)	5.716 (6.475)	1.142 (0.074)	315
Al_2O_3 Fe – AM	0.027 (0.084)	0.296 (0.314)	0.076 (0.055)	0.170 (0.128)	5.337 (5.107)	1.149 (0.071)	757
Al_2O_3 Fe – BD	0.048 (0.167)	0.367 (0.387)	0.095 (0.080)	0.207 (0.175)	5.723 (5.910)	1.142 (0.075)	818

Analysis of the processed FE-SEM images, has demonstrated submicron Al_2O_3 Fe particle sizes achieved by the sol-gel technique. The mean diameter (D_{mean}) of neat Al_2O_3 Fe particles was 0.171 ± 0.123 µm (Table 2). Obtained high standard deviations (with values close to the mean) indicate broad distribution of particle size in a wide diameter range. The obtained

diameter ranges by image analysis were 0.007 – 2.119 µm for neat Al_2O_3 Fe particles; 0.008 – 2.623 µm for Al_2O_3 Fe – VT; 0.010 – 3.355 µm for Al_2O_3 Fe – ME; 0.009 – 3.255 µm for Al_2O_3 Fe – AM; and 0.013 – 4.351 µm for Al_2O_3 Fe – BD. Still, the predominance of smaller particles led to small mean diameters (Table 2).

Surface modification by VT induced a decrease in the surface area and particle diameter, while that by BD increased the particle size, which was shown later to lead to a weaker reinforcement. Thus, the surface modification type influences particle agglomeration and consequently the apparent particle size, where lower agglomeration leads to better composite reinforcement.

10.2 FTIR CHARACTERIZATION OF FILLERS AND COMPOSITE FILMS

FTIR spectra of neat Al_2O_3 Fe particles as well as particles with surface modifications (MEMO, VTMOEO, APTMS and BD) are shown in Figure 24.
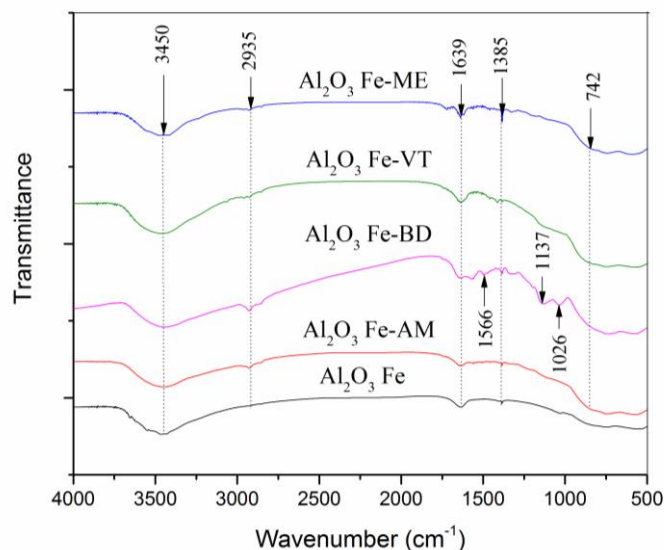
Figure 24 Comparison of FTIR spectra of Al_2O_3 Fe based particles used in composites preparation.

The characteristic peaks of investigated particles observed at 3460 cm^{-1} can be assigned to O-H groups [82]. The following peak at ~1639 cm^{-1} relates to the H_2O vibrational bending mode [83,84]. Absorption at 740 cm^{-1} could be attributed to vibrational modes associated with $[M^{II,III}(OH)_6]^{4-,3-}$ complexes distributed along the double hydroxide (LDH) layers mostly attributed to the γ crystalline [85] structure of alumina [86,87].

Introduced surface functionality on the particles has led to the emergence of new peaks. The peaks at 2935 cm^{-1} are attributed to the ethylene C-H stretching bands of attached silane. The peaks at 1636/1639 cm^{-1} showed skeletal C=C double bond vibrations from silane functional groups at MEMO modified particles that overlapped with H_2O vibrational bending mode.

10.3 Micro hardness of composites having surface modified alumina fillers

Micro hardness of prepared composites with two different modifications of alumina based particles is presented in Figure 25. The micro hardness of composites increases with increasing the amount of fillers. The pure polymer film has the micro hardness of 0.1881 GPa and the composite with the ferrous oxide doped alumina particles with different modifications (MEMO and VTMOEO) has the best resistance to indentation the hardness is improved significantly with addition of filler particles. The micro hardness of composites with addition of 3 wt. % of modifications filler increases from 58 % to 97 % compared to the pure matrix material depending on the type of modifications of fillers. The hardness of the samples with 3 wt. % with modified (VTMOEO) particles is better than the hardness of the composite with 10 wt. % non-modified particles [72]. A significant increase in hardness indicates that in the modified particles enables the good improvement of mechanical properties with lower content of particles.
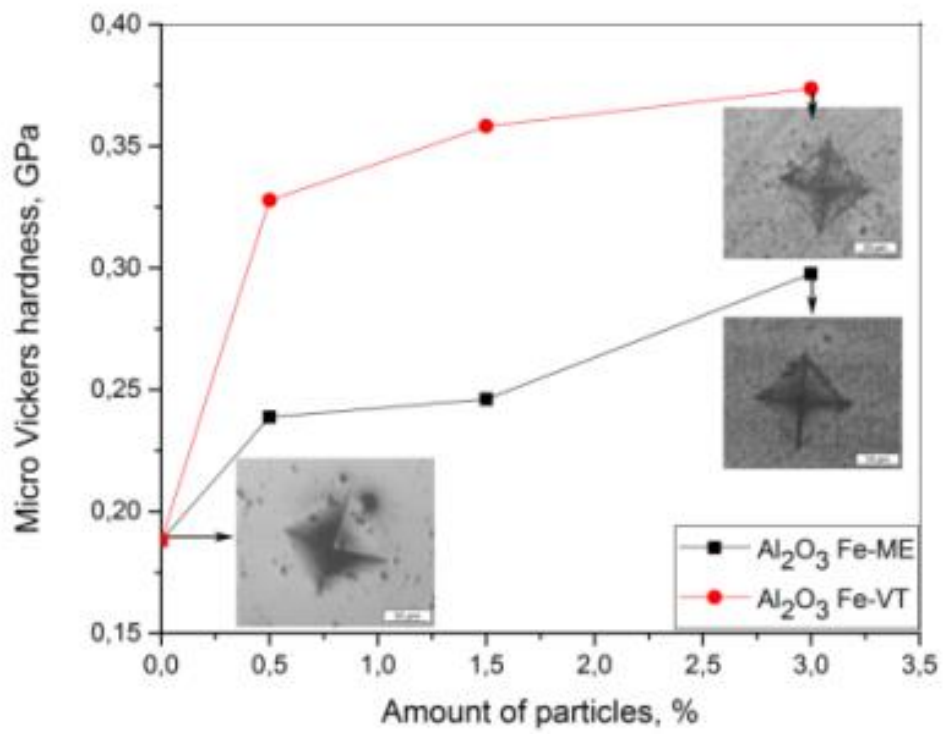
Figure 25 Microhardness of two composites having different filler modifications
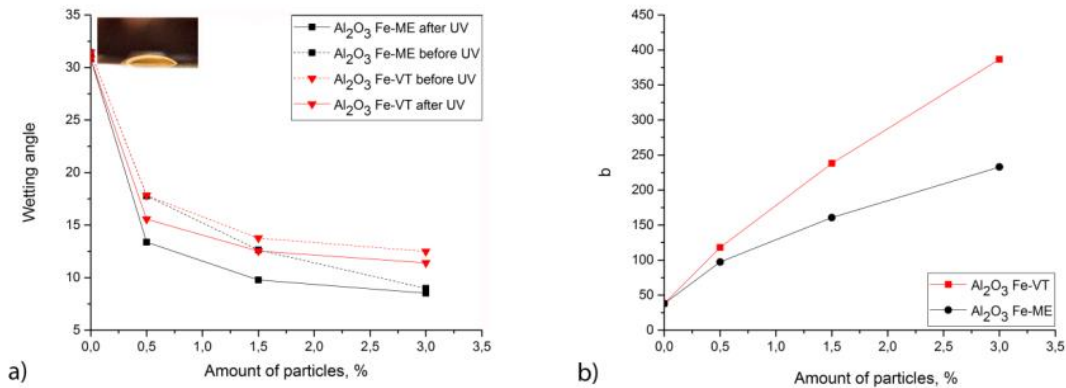
Figure 26 a) Micro hardness changes regarding the amount of different modifications (MEMO and VTMOEO) of ferrous oxide doped alumina based particles, b) wetting angle for composite films before and after UV curing, c) the dependence of the adhesion strength parameter b of the particles share.

The contact angles of composite filed using differently modified ferrous oxide doped alumina particles decreased with increasing the share of particles in the composite. Decrease of contact angle for different composite films is obvious in Figure 2b. The measured contact angles are presented in function of a particles share in the composite. Low contact angle enables good wetting and then the adhesive flows into the valleys and crevices on the metal surface. Higher contact angle results in poor wetting when the adhesive bridges over the valleys and results in a reduction of the actual contact area between the adhesive and the adhered, resulting in a lower overall joint strength88 . The apropriate mathematical model was used to evaluate the adhesion from the series of microhardness measurements by calculation of the factor *b* that represents the level of the adhesion between the substrate and the film trough the specific parameter b, representing the ratio of the radius of the plastic zone under indenter and depth of indentation and it changes depending on the combination of the film and the substrate and adhesion between them.

10.3.1 Investigation of cavitation erosion of films reinforced with surface modified alumina based particles

During the cavitation experiment, mass losses of dried samples were found (Figure 27). The obtained data enable comparison of mass losses in composite films with modified particles to those, previously reported [72] where much higher contents of particles were used to obtain similar result.
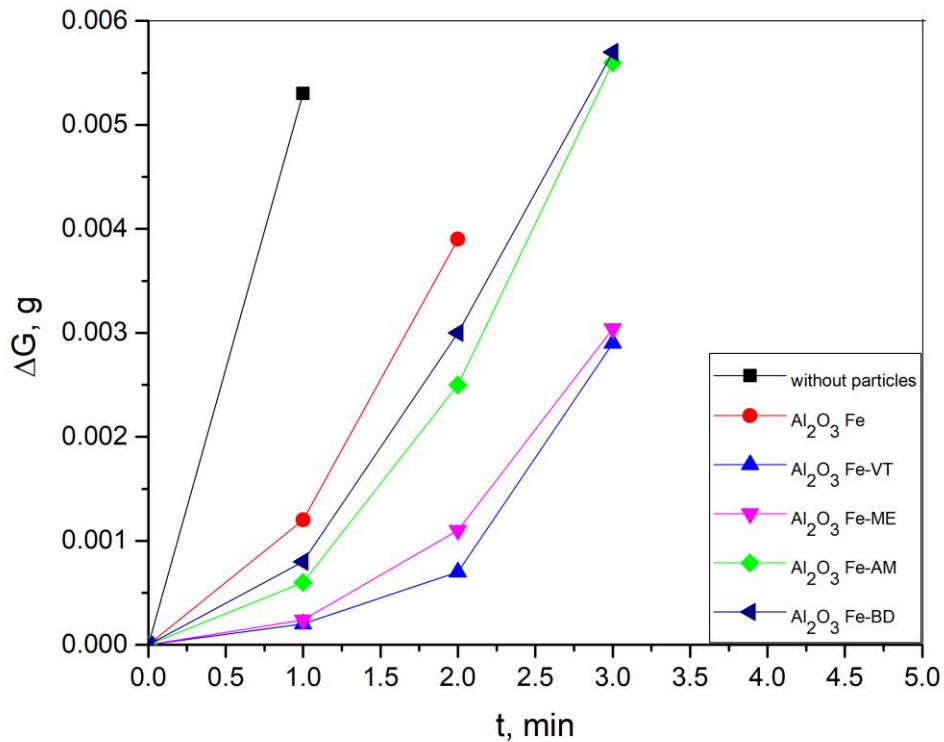
Figure 27 Mass loss during cavitation resistance testing for pure composite films and composite films with 3 wt. % of different alumina based particles.

Pure polymer films are not very resistant to cavitation as they get destructed after only 1 min of testing. The addition of ferrous doped alumina fillers increases this time to 2 min and lowers the destruction rate represented as the lower rate of mass loss of the specimen. When the filler particles were modified, reinforced composite is obtained with improved adhesion to the substrate. Every modified film behaved better than the pure polymer in terms of longevity. The VT and ME films exhibit longer film exposure times as well as a significantly lower mass loss during the whole testing period. Behavior of these films is better in terms of mass loss due to cavitation as well as of the film durability. The VT and ME modifications can be considered as a successful mean for enhancing both cavitation resistance and adhesion to the metal substrate.

Mass loss for the composite film having the best cavitation resistance with a ferrous oxide doped alumina based particles with VT surface modification having different filler contents is presented in Figure 28. It can be observed that the addition of 3 wt. % of the modified filler significantly improves the cavitation resistance of the film. The adhesion of this film should be significantly better as compared to the pure polymer film. On the contrary, addition of 0.5 as well as 1.5 wt. % of the filler does not seem to be sufficient to improve the cavitation resistance of the composite film.
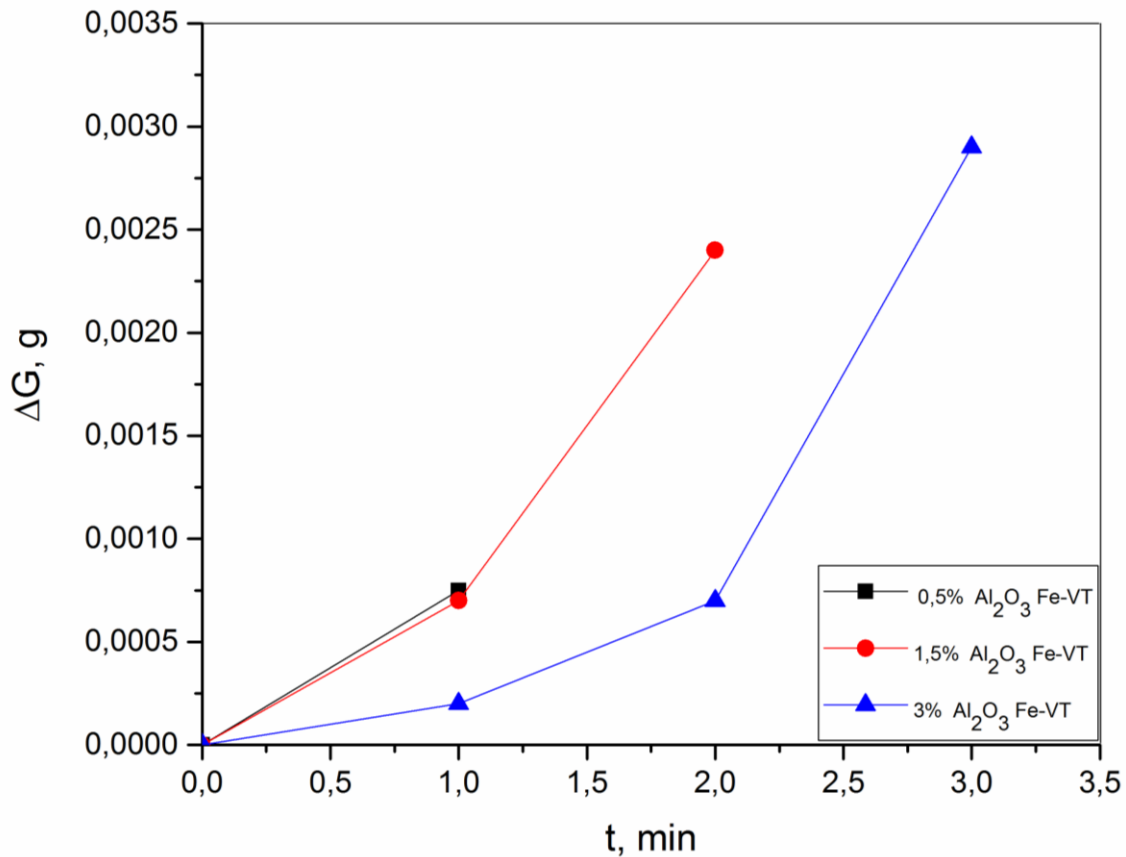
Figure 28 Mass loss during cavitation resistance testing for composite films reinforced with Al₂O₃ Fe –VT.

10.3.2 Image analysis of cavitation damages

Imaging of the cavitation damage was done using the surface scanner. The scanner enables the resolution of 600 points / 2.52 cm which is good enough to visualize very small defects. The surface was colored in black at the beginning of the experiment in order to enable visualization on the normally transparent film. The obtained images had very small difference in grey level between the damaged and not damaged parts and therefore the images were subjected to the image analysis tools. The software used was image pro plus, and the technique that enables to distinguish between 256 levels of grey. Human eye is able to see

only 32 levels of grey so this technique was the way to get information about the very fine levels of grey difference that correspond to the destruction, but which are invisible to the naked eye. The technique used is called bitmap analysis and corresponds to the measurement of the grey level of every point in the obtained image.

Images showing surface defects after 1 min of cavitation for samples made of composite films with 0.5 wt. % of different alumina based particles are shown in Figure 29.
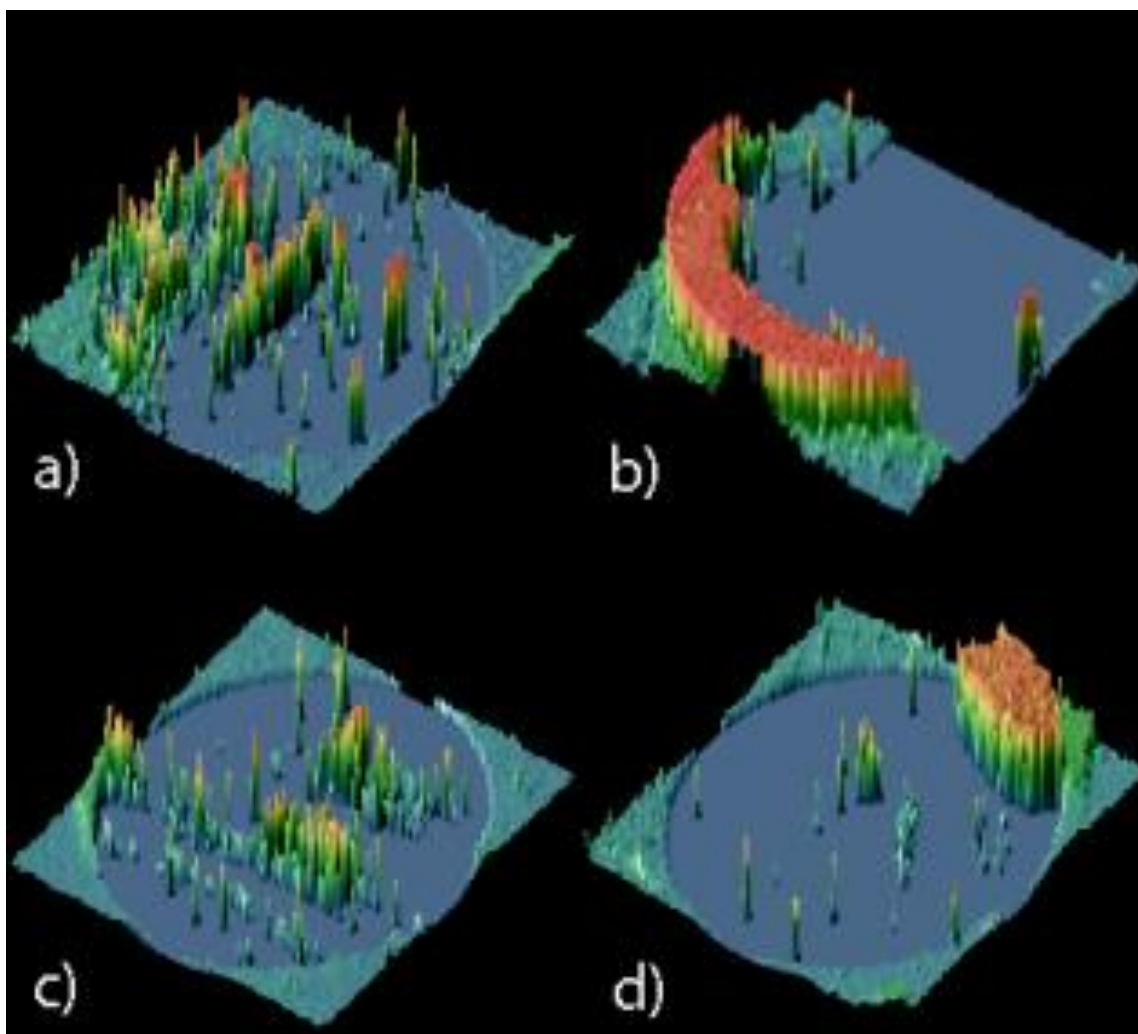
Figure 29 Surface plot images after 1min of cavitation for composite films with: a) 0.5 wt. % of Al₂O₃ Fe − AM, b) 0.5 wt. % of Al₂O₃ Fe − BD, c) 0.5 wt. % of Al₂O₃ Fe − ME and d) 0.5 wt. % of Al₂O₃ Fe − VT.

The Image Pro Plus program was used for determination of the surface deterioration level. The part of the damaged surface was measured using image analysis tools and the obtained result is presented in Figure 30.
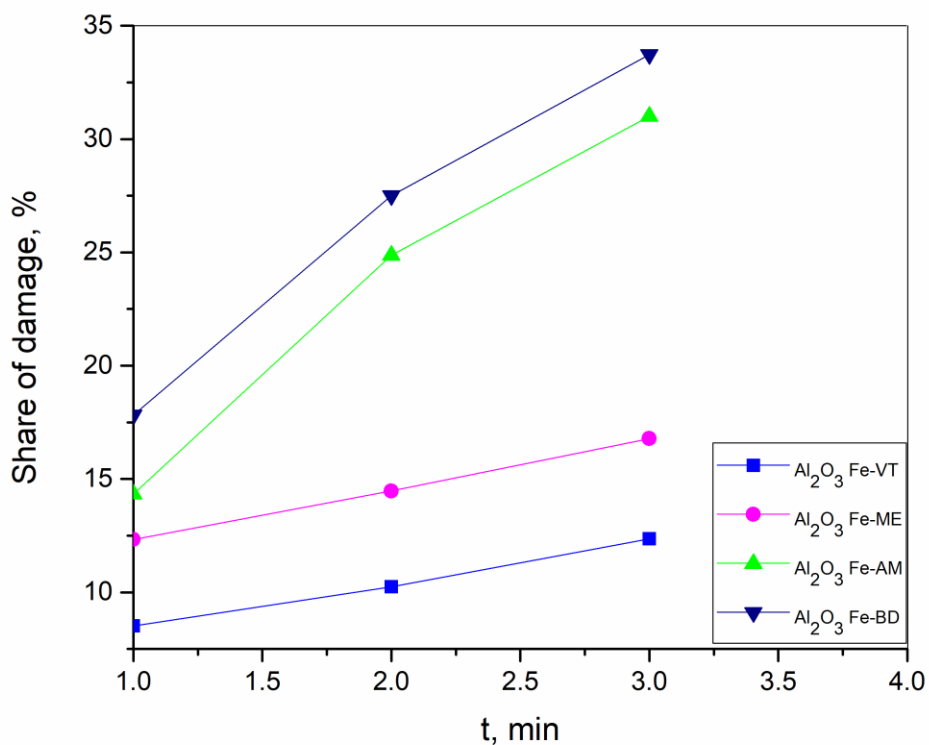
Figure 30 Share of observed damage to composite films vs. time for samples with 0.5 wt. % of different alumina based particles.

The surface degradation is considerable in the film with BD modified fillers,, which is in accordance with mass loss measurements. The film with ME modified particles behaves better in terms of mass loss, but the surface degradation level is comparable to that with the BD modified filler. The mass loss of this composite is lower as compared to the composite with AM modified fillers, which exhibits better surface resistance in terms of the surface

damage ratio. These findings could be related to the size of defects observed in images of composite films after exposure to cavitation. The ME film exhibit larger damaged areas, but the depth of those damages remains lower. The best performance in terms of the surface degradation level, as well as in terms of mass loss, has the composite with VT modified fillers. The overall surface destruction share after 3 min. shows that at the end of the testing procedure the BD modified films have the highest surface degradation level of about ~33.7 % while the surface degradation level is the lowest in VT modified films amounting to ~12.3 %.

10.3.3 Optical microscopy for visualization of adhesion of films composed of acrylate reinforced with surface modified alumina particles

Cross sections of films after cavitation, for the composite film reinforced with Al_2O_3 Fe – VT, exhibiting the best adhesion and the cross section of the film reinforced with Al_2O_3 Fe – BD exhibiting the weakest adhesion, are shown in Figure 31 .
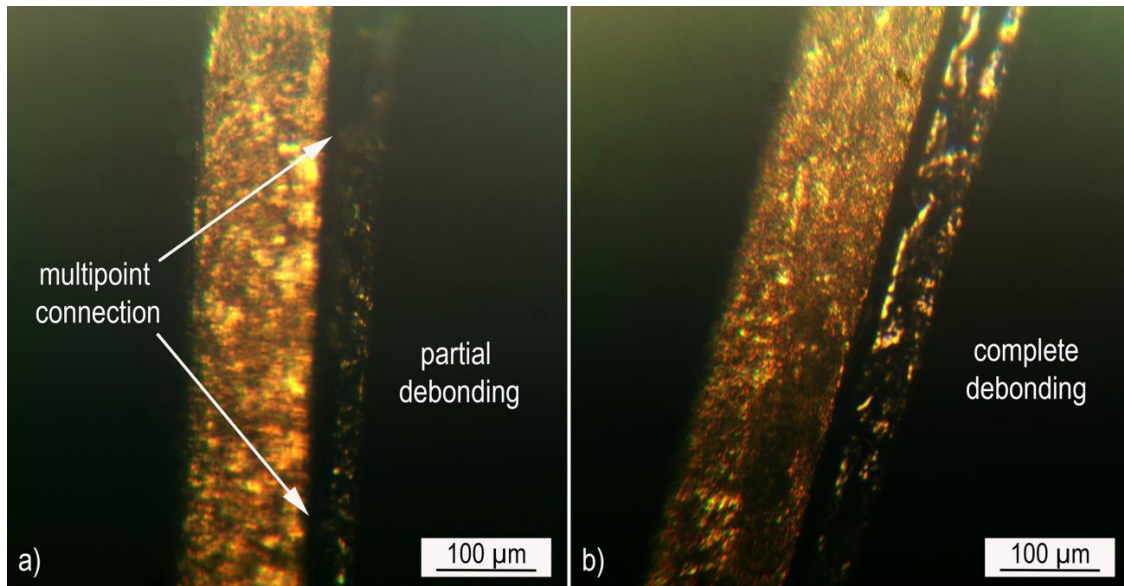
Figure 31 Cross-sections of composite films after the cavitation test, reinforced with: a) Al_2O_3 Fe – VT and b) Al_2O_3 Fe – BD particles

It can be seen that the latter composite film almost completely debonded from the substrate (Figure 31). On the contrary, the composite film reinforced with Al_2O_3 Fe – VT particles resisted to the cavitation erosion by stronger adhesion, which is seen by remaining multipoint connection to the substrate and the lowest share of damage.

11 Visualization of adhesion using hardness testing

The measurement of the indent size is done using the image analysis software. The observation of the indent aspect gives opportunity to obtain the information about the adhesion quality visually, only from data obtained using the quantification of the indent image. The depth of the indent can be evaluated from the bitmap analysis that enables the estimation of the shape of the hole on the surface of the film. It was observed that the better the adhesion is, the indentation produces the damage on the surface that goes straight into the material and leaves indent that corresponds closely to the shape of the indenter. The obtained images were processed and the estimated indent shape gives indent in the composite produced using the ME modified fillers much larger than that obtained using the VT modified filler that presents better adhesion properties.
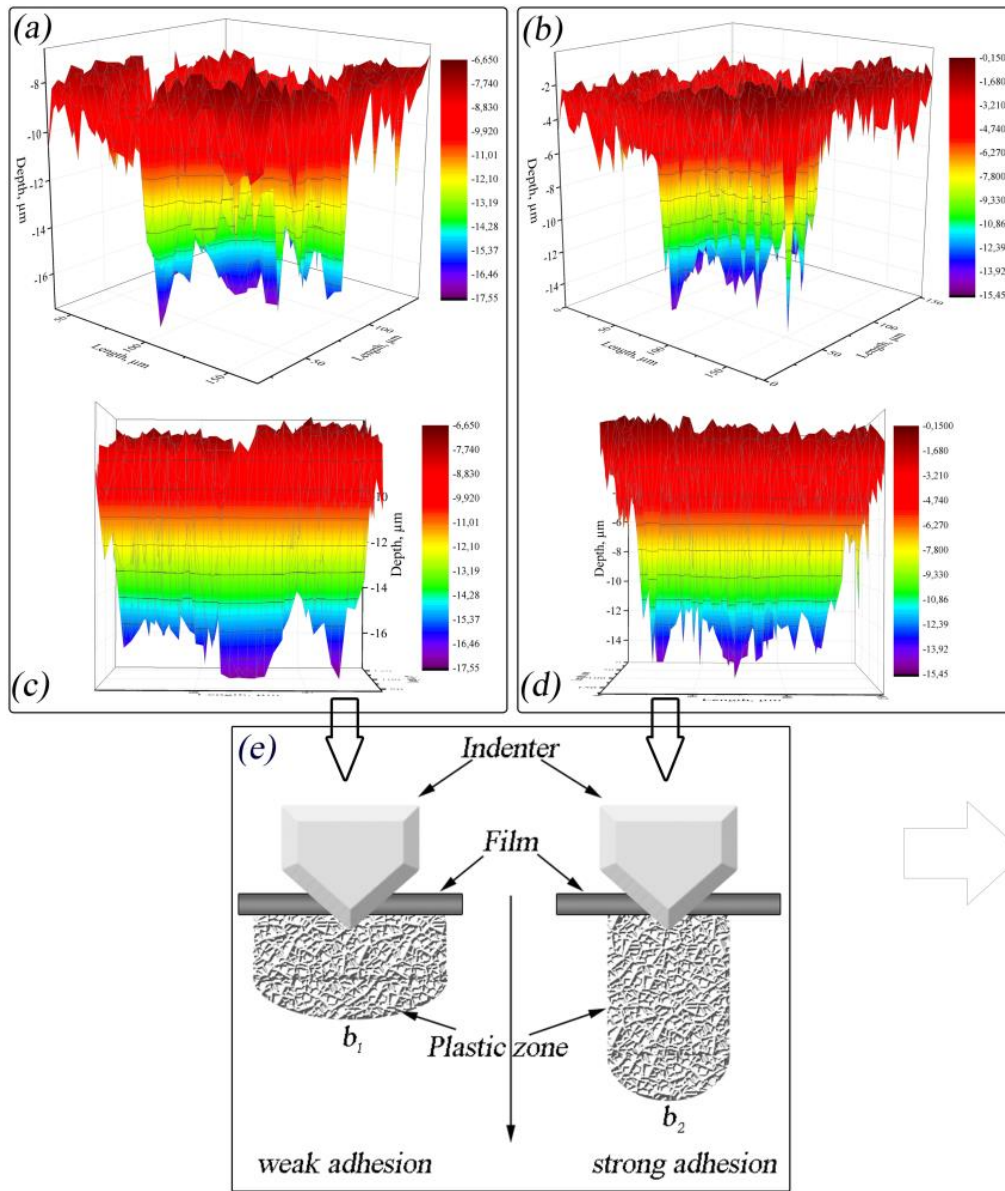
Figure 32   a) 3 wt. % VT, b) 3 wt. % VT, c) 3 wt. % ME, d) 3 wt. % ME, and (e) Schematic representation of deformation associated with indentation in a coated substrate (weak adhesion and strong adhesion).

12 CONCLUSION

The theoretical part of the thesis opened the topics to be addressed in the experimental part and results. The introduction part deals with the materials science connected to dentistry and the main postulates of solving problems in materials science.

In theoretical part the main topics treated in the dissertation are addressed starting from polymer materials used in dentistry and their specifications, the composite materials are considered with special view on materials used in dentistry. Finally the adhesive systems and their development are presented in a separate chapter as they are important part of the thesis. In theoretical part the methods of characterization used in the materials characterization are presented.

Experimental part is presenting three groups of results. The first one addresses the problem about how to measure adhesion of a system that is supposed to be very strong but the polymer dissolves in most of the glues used in standard procedures to measure adhesion using the pull test. So adhesion was measured indirectly using the micro hardness testing and those results gave consisting results. In order to prove those results the measurement of contact angle was added to the procedure and they were in accordance. As the conditions in which the adhesives operate the film of a proposed adhesive was subjected to cavitation process to measure the adhesion. All the results were in accordance showing that the particles synthesized for this purpose that were alumina based particles and ferrous oxide doped alumina particles improve adhesion of the film. The properties of the film were also improved with the addition of the reinforcement.

As the adhesion to the metal substrate is difficult to achieve the particles were further surface modified to obtain improved adhesion properties. The particles were modified using the surface modification by VT that induced a decrease in the surface area and particle diameter, while that by BD increased the particle size, which was shown later to lead to a weaker reinforcement. Thus, the surface modification type influences particle agglomeration and

consequently the apparent particle size, where lower agglomeration leads to better composite reinforcement. Both improvements of surface structure were suitable for the improvement of adhesion of the film.

The final contribution in this thesis is linked to the visualization of adhesion. It was seen that the better the adhesion is the image obtained under the indenter changed. Better adhesion could also be visually estimated from the image analysis. This observation was proved for the tested surface modified particles used as reinforcing agents.

The adhesive systems could be improved using nonmodified alumina based particles and their interaction with the polymer matrix as well as the interaction with the metal surface showed the improvement of adhesion properties. Further improvement was obtained using the modified particles as adhesion was improved with smaller content of the reinforcement compared to particles with no surface modification.

LITERATURE

[1] M. Roach. Base metal alloys used for dental restorations and implants. Dent Clin North Am 2007; 51: 603 – 27.

[2] M. Saini, Y Singh, P Arora, MN KLumar. Implant biomaterials: A comprehensive review. World J Clin Cases 2015; 3: 52 – 7.

[3] M. Navarro, A. Michiardi, O. Castaño, J. A. Planell. Biomaterials in Orthopaedics. J R Soc Interface 2008; 5: 1137–58

[4] T. M. Muffly, A. P. Tizzano, M. D Walters, The history and evolution of sutures in pelvic surgery, J R Soc Med, 2011; 104 (3): 107-112

[5] M. F. Maitz, Applications of synthetic polymers in clinical medicine, Biosurface and Biotribology, 2015; 1 (3): 161-176

[6] C. Slack. Noble obsession: Charles Goodyear, Thomas Hancock, and the race to unlock the greatest industrial secret of the nineteenth century. Hyperion (2002). ISBN 978-0-7868-6789-9.

[7] D. Hosler, S. L. Burkett; M. J. Tarkanian, Prehistoric polymers: Rubber processing in ancient Mesoamerica. Science 1999; 284 (5422): 1988–1991

[8] J. L. Meikle, American Plastic: A Cultural History. New Brunswick, NJ: Rutgers University Press (1995). ISBN 0-8135-2235-8.

[9] M. F. Maitz, Applications of synthetic polymers in clinical medicine. Biosurf Biotribol 2015; 1: 161–76

[10] P. A. Leggat, D. R. Smith, U. Kedjarune, Surgical applications of methyl methacrylate: a review of toxicity, Arch. Environ. Occup. Health 2009; 64: 207–212.

[11] M. Tanaka, A. Mochizuki, Clarification of the blood compatibility mechanism by controlling the water structure at the blood–poly(meth) acrylate interface, J. Biomater. Sci. Polym. Ed. 2010; 21: 1849–1863.

[12] M. Tanaka, T. Motomura, M. Kawada, T. Anzai, Y. Kasori, T. Shiroya, K. Shimura, M. Onishi, A. Mochizuki, Blood compatible aspects of poly (2-methoxyethylacrylate) (PMEA) – relationship between protein adsorption and platelet adhesion on PMEA surface, Biomaterials 2000; 21: 1471–1481.

[13] S. H. Kim, A. Opdahl, C. Marmo, G. A. Somorjai, AFM and SFG studies of pHEMA-based hydrogelcontact lens surfaces in saline solution: adhesion, friction, and the presence of non-crosslinked polymer chains at the surface, Biomaterials, 2002; 23: 1657–1666.

[14] S. Klapdohr, N. Moszner, New inorganic components for dental filling composites, Monatsh. Chem. 136 (1) (2005) 21‑45.

[15] J.W. Kim, L.U. Kim, C.K. Kim, B.H. Cho, O.Y. Kim, Characteristics of novel dental composites containing 2,2-bis[4-(2-methoxy-3-methacryloyloxy propoxy) phenyl] propane as a base resin, Biomacromolecules 7 (1) (2006) 154–160.

[16] R. Braga, R. Ballester, J. Ferracane, Factors involved in the development of polymerization shrinkage stress in resin-composites: a systematic review, Dent. Mater. 21 (10) (2005) 962‑970.

[17] M. Dewaele, D. Truffier-Boutry, J. Devaux, G. Leloup, Volume contraction in photocured dental resins: the shrinkage-conversion relationship revisited, Dent. Mater. 22 (4) (2006) 359‑365.

[18] B.A.M. Venhoven, A.J. de Gee, C.L. Davidson, Polymerization contraction and conversion of light-curing BisGMA-based methacrylate resins, Biomaterials 14 (11) (1993) 871‑875.

[19] S. Yuan, F. Liu, J. He, Preparation and characterization of low polymerization shrinkage and bis-GMA-free dental resin system: research article, Adv. Polym.

Technol. 34 (3) (2015) (n/a-n/a).

[20] K. K. Chawla, Composite Materials: Science and Engineering, Springer-Verlag New York, 2012, ISBN 978-1-4757-3914-5 DOI 10.1007/978-1-4757-3912

[21] S. Hogmark, S. Jacobson, M. Larsson, Design and evaluation of tribological coatings, Wear 2000; 246 (1-2): 20-33

[22] Omar Alageel, Mohamed-NurAbdallah, ZhongYuanLuo, Jaime Del-Rio-Highsmith, MartaCerruti, FalehTamimi, Bonding metals to poly(methyl methacrylate) using aryldiazonium salts, dental materials 31 (2015) 105–114

[23] Matsuda Y, Yanagida H, Ide T, Matsumura H, Tanoue N. Bond strength of poly(methyl methacrylate) denture base material to cast titanium and cobalt–chromium alloy. J Adhes Dent 2010;12:223–9.

[24] Rothfuss LG, Hokett SD, Hondrum SO, Elrod CW. Resin to metal bond strengths using two commercial systems. J Prosthet Dent 1998;79:270–2.

[25] Brantley WA, Eliades T. Orthodontic materials cientific and clinical spects. Stuttgart, NewYork, NY: Thieme; 2001.

[26] Sakaguchi RL, Powers JM. Craig's restorative dental materials. St. Louis, Mo: Elsevier/Mosby; 2012.

[27] T. K. Vaidyanathan, J. Vaidyanathan, Recent Advances in the Theory and Mechanism of Adhesive Resin Bonding to Dentin: A Critical Review. Inc. J Biomed Mater Res Part B: Appl Biomater. 2009; 88: 558–578

[28] E. Sofan, A. Sofan, G. Palaia, G. Tenore, U. Romeo, G. Migliau, Classification review of dental adhesive systems: from the IV generation to the universal type, Ann Stomatol (Roma). 2017; 8(1): 1–17.

[29] K. L. Van Landuyt, J. Snauwaert, J. De munck, M. Peumans, Y. Yoshida, A. Poitevin, et al., Systematic review of the chemical composition of contemporary dental adhesives. Biomaterials. 2007; 28: 3757–3785.

[30] J. Perdigão, New developments in dental adhesion. Dent Clin North Am. 2007; 51: 333–357.

[31] A. H. Susin, W. A. Vasconcellos, J. R. Saad, O. B. Oliveira Junior. Tensile bond strength of self-etching versus total-etching adhesive systems under different dentinal substrate conditions. Braz Oral Res. 2007; 21(1): 81–86.

[32] J. Perdigão, Dentin bonding-variables related to the clinical situation and the substrate treatment. Dent Mater. 2010; 26: 24–37.

[33] K. J. Söderholm, Dental adhesives how it all started and later evolved. J Adhes Dent. 2007; 9(2): 227–230.

[34] J. W. Mclean, I. R. H. Kramer, A clinical and pathological evaluation of a sulphinic acid-activated resin for use in restorative dentistry. Br Dent J. 1952; 93: 255–269.

[35] M. Buonocore, A simple method of increasing the adhesion of acrylic filling materials to enamel surfaces. J Dent Res. 1955; 34: 849–853.

[36] M. Buonocore, A. Marsui, A. J. Gwinnett, Penetration of resin dental materials into enamel surfaces with reference to bonding. Arch Oral Biol. 1968; 13(1): 61–70.

[37] E. Jr Swift, J. Perdigao, H. Heymann, Bonding to enamel and dentin: a brief history and state of the art. Quintessence Int. 1995; 26: 95–110.

[38] A. Sezinando, Looking for the ideal adhesive – A review. Rev port Estomatol Med Dent Cir Maxilofac. 2014; 4: 194–206.

[39] J. Eick, R. Wilko, C. Anderson, S. Sorensen, Scanning electron microscopy of cut tooth surfaces and identification of debris by use of the electron microprobe. J Dent Res. 1970; 49: 1359–1368.

[40] N. Nakabayashi, K. Kojima, E. Masuhara, The promotion of adhesion by the infiltration of monomers into tooth substrates. J Biomed Mater Res. 1982; 16(3): 265–273.

[41] De Munck J, Van Landuyt K, PeumansM, et al. A critical review of the durability of adhesion to tooth tissue: methods and results. J Dent Res. 2005;84:118-132.
[42] Breschi L, Mazzoni A, De Stefano D, Ferrari M. Adhesion to intraradicular dentin: a review. J Adhes Sci Technol. 2009; 7:1053e83.

[43] H. Lu, Y. Liu, W. M. Huang, C. Wang, D. Hui, Y. Q. Fu, Controlled evolution of surface patterns for ZnO coated on stretched PMMA upon thermal and solvent treatments. Compos B Eng 2018; 132: 1–9.

[44] D. E. Packman, Handbook of Adhesion Second Edition, John Wiley & Sons, 2006.

[45] H. Ollendorf, T. Schulke, D. Schneider, Testing the adhesion of hard coatings including the non-destructive technique of surface acoustic waves, Adhesion Measurement of Films & Coatings 2001; 2: 49-77.

[46] J. Kajohnchaiyagual, C. Jubsilp, I. Dueramae, S. Rimdusit, Thermal and mechanical properties enhancement obtained in highly filled alumina-polybenzoxazine composites. Polym Comp 2014; 35(11): 2269-2279.

[47] J. Suwanprateeb, A Comparison of Different Methods in Determining Load- and Time-Dependence of Vickers Hardness in Polymers, Polym Test 1998; 17: 495–506.

[48] M. Chen, J. Gao, The adhesion of copper films coated on silicon and glass substrates, Mod Phys Lett B 2000; 14: 103-108.

[49] D. Chicot, J. Lesage, Absolute hardness of films and coatings, Thin Solid Films 1995; 254: 123 – 130.

[50] P. J. Burnett, D. S. Rickerby, The Mechanical Properties of Wear resistant coatings I. Modelling of Hardness Behaviour, Thin Solid Films 1987; 148: 41-50.

[51] J. R. Tuck, A.M. Korsunsky, R. I. Davidson, S. J. Bull, D. M. Elliott, Modelling of the hardness of electroplated nickel coatings on copper substrates, Surf Coat Tech 2000; 127: 1 – 8.

[52] E. S. Puchi-Cabrera, A new model for the computation of the composite hardness of coated systems, Surf Coat Tech 2002; 160: 177–186.

[53] F. Kawano, T. Ohguri, T. Ichikawa, I. Mizuno, A. Hasegawa, Shock absorbability and hardness of commercially available denture teeth. Int J Prosthodont 2002; 15: 243–7.

[54] N. Tanoue, H. Matsumura, M. Atsuta, Effectiveness of polymerization of a prosthetic composite using three polymerization systems, J Prosthet Dent 1999; 82: 336–40.

[55] Y. Abe, Y. Sato, Y. Akagawa, S. Ohkawa, An in vitro study of high-strength resin posterior denture tooth wear. Int J Prosthodont 1997; 10: 28–34.

[56] G. L. García, V. López-Ríosb, A. Espinosaa, J. Abenojarc, F. Velascoc, A. Toro, Cavitation resistance of epoxy-based multilayer coatings: Surface damage and crack growth kinetics during the incubation stage, Wear 2014; 316: 124–132.

[57] A. Chiche, J. Dollhofer, C. Creton, Cavity growth in soft adhesives, Eur. Phys. J. E 2005; 17: 389–401.

[58] D. E. Packham, Work of adhesion: contact angles and contact mechanics, Int J Adhes Adhes 1996; 16: 121-128.

[59] A. Sklodowaka, M. Wozniak, R. Matlakowska, The method of contact angle measurements and estimation of work of adhesion in bioleaching of metals, Biol Proced Online 1999; 1: 114–121.

[60] R. D. Hazlett. Fractal applications: Wettability and contact angle, J Colloid Interf Sci 1990; 137: 527-533.

[61] S. Ebnesajjad, A. H. Landrock, Adhesives Technology Handbook, Elsevier Inc., London, UK, 2015.

[62] A. Akinci, S. Sen, U. Sen, Friction and wear behavior of zirconium oxide reinforced PMMA composites, Composites: Part B 2014; 56: 42–47

[63] S.-L. Bee, M.A.A. Abdullah, M. Mamat, S.-T. Bee, L. T. Sin, D. Hui, et al. Characterization of silylated modified clay nanoparticles and its functionality in PMMA. Composites Part B 2017;110: 83–95.

[64] Y. Abe, Y. Sato, Y. Akagawa, S. Ohkawa, An in vitro study of high-strength resin posterior denture tooth wear, Int J Prosthodont 1997; 10: 28–34.

[65] L. D. Randolph, W. M. Palin, G. Lelou, J. G.Leprince, Filler characteristics of modern dental resincomposites and their influence on physico-mechanical properties. Dent Mater 2016; 32: 1586–99.

[66] Marina Dojcinovic, Tatjana Volkov-Husovic, Cavitation damage of the medium carbon steel: Implementation of image analysis, Materials Letters 62 (2008) 953–956
[67] J. L. He, W. Z. Li, H. D. Li., Hardness measurement of thin films: Separation from composite hardness, Appl. Phys. Lett. 1996; 69: 1402.

[68] M. B. Posarac-Markovic, Dj. N. Veljovic, A. B. Devecerski, B. Z. Matovic, T. D. Volkov-Husovic, Nondestructive evaluation of surface degradation of silicon carbide – cordierite ceramics subjected to the erosive wear, Mater Design 2013; 52: 295–9.

[69] L. Magagnin, R. Maboudian, C. Carraro, Adhesion evaluation of immersion plating copper films on silicon by microindentation measurements. Thin Solid Films 2003; 434: 100–5.

[70] Jeol User's Manual, https://www.jeol.co.jp/en/

[71] B. Herman, J. J. Lemasters (eds.), Optical Microscopy: Emerging Methods and Applications Academic Press, New York,1993, pp 441

[72] A. A. Algellai, N. Tomić, M. M. Vuksanović, M. Dojčinović, T. Volkov Husović, V. Radojević, R. Jančić Heinemann, Adhesion testing of composites based on Bis-GMA/TEGDMA monomers reinforced with alumina based fillers on brass substrate, Compos Part B – Eng. 2018; 140: 164–173.

[73] J. Zec, N. Tomić, M. Zrilić, S. Marković, D. Stojanović, R. Jančić-Heinemann, Processing and characterization of UHMWPE composite fibres with alumina particles in poly(ethylene-vinyl acetate) matrix, J Thermoplas Compos. 2017; 31: 689–708.

[74] F. A. Alzarrug, M. M. Dimitrijević, R. M. Jančić Heinemann, V. Radojević, D. B. Stojanović, P. S. Uskoković, R. Aleksić, The use of different alumina fillers for improvement of the mechanical properties of hybrid PMMA composites, Mater Design, 2015, 86: 575-581

[75] M. Sadej, E. Andrzejewska, Silica/aluminum oxide hybrid as a filler for photocurable composites, Progress Organ. Coat.2016; 94: 1–8

[76] S. A. B. Hassan, M. M. Dimitrijevic, A. M. Kojovic, D. B. Stojanovic, K. Obradovic-Djuricic, R. M. Jancic-Heinemann, R. R. Aleksic, The effect of the size and shape of alumina

nanofillers on the mechanical behavior of PMMA matrix composites, Journal of the Serbian Chemical Society, 2014; 79 (10): 1295-1307

[77] G. Zu, J. Shen, X. Wei, X. Ni, Y. Zhang, J. Wang, G. Liu, Preparation and characterization of monolithic alumina aerogels. J Non Cryst Solids 2011; 357: 2903–2906.

[78] D-Y. Li, Y-S. Lin, Y-C. Li, et al, Synthesis of mesoporous pseudoboehmite and alumina templated with 1-hexadecyl-2,3-dimethyl-imidazolium chloride. Microporous Mesoporous Mater 2008; 108: 276–282.

[79] V. Natarajan, J. Kalyana Sundar, P. Selvarajan, M. Arivanandhan, K. Sankaranarayanan, S. Natarajan, Y. Hayakawa, Crystal Growth, Thermal, Mechanical and Optical Properties of a New Organic Nonlinear Optical Material: Ethyl P-Dimethylamino Benzoate (EDMAB), J Miner Mater Char Engin 2011; 10: 1-11.

[80] A. B. Denis, C. A. Diagone, A. M. G. Plepis, R. B. Viana, Kinetic Parameters during Bis-GMA and TEGDMA Monomer Polymerization by ATR-FTIR: The Influence of Photoinitiator and Light Curing Source, J Spectrosc 2016; 2016: 1-8.

[81] W. Possart, Experimental and theoretical description of the electrostatic component of adhesion at polymer/metal contacts, Int J Adhes 1988; 8: 77.

[82] M. A. Ulibarri, M. J. Hernandez, J. Cornejo, Hydrotalcite-like compounds obtained by anion exchange reactions, J Mater Sci. 1991; 26: 1512–1516.

[83] I. E. Grey, R. Ragozzini, Formation and characterization of new magnesium aluminum hydroxycarbonates, J Solid State Chem. 1991; 94: 244–253.

[84] G. Abellán, E. Coronado, C. Martí-Gastaldo, E. Pinilla-Cienfuegos, A. Ribera, Hexagonal nanosheets from the exfoliation of Ni^{2+}-Fe^{3+} LDHs: a route towards layered multifunctional materials, J Mater Chem. 2010; 20: 7451–7455.

[85] M. Pracella, M. M. U. Haque, V. Alvarez, Compatibilization and properties of EVA copolymers containing surface-functionalized cellulose microfibers, Macromol Mater Eng. 2010; 295: 949–957.

[86] A. Drah, N. Tomić, Z. Veličić, A. D. Marinković, Ž. Radovanović, Z. Veličković, R. Jančić-Heinemann, Highly ordered macroporous γ-alumina prepared by modified solgel method with PMMA microsphere template for enhanced Pb^{2+}, Ni^{2+} and Cd^{2+} removal, Ceram Int. 2017; 43: 13817–13827.

[87] G. Busca, F. Trifiro, A. Vaccari, Characterization and catalytic activity of cobalt-chromium mixed oxides. Langmuir. 1990; 6: 1440–1447.

[88] S. Ebnesajjad, A. H. Landrock, Adhesives Technology Handbook, Elsevier Inc., London, UK, 2015.

Прилог 1.

Изјава о ауторству

Потписани-а <u>Ahmed Algellai</u>
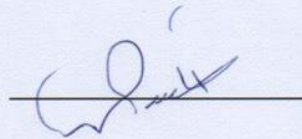
број индекса _____

Изјављујем

да је докторска дисертација под насловом

„Adheziona svojstva fotopolimerizujućih kompozitnih filmova na bazi metakrilata i čestica aluminijum oksida za primenu u stomatologiji", „Adhesion properties of UV-curing methacrylate - alumina particles composite films for use in dentistry"

- резултат сопственог истраживачког рада,
- да предложена дисертација у целини ни у деловима није била предложена за добијање било које дипломе према студијским програмима других високошколских установа,
- да су резултати коректно наведени и
- да нисам кршио/ла ауторска права и користио интелектуалну својину других лица.

Потпис докторанда

У Београду, 25.6.2017

Прилог 2.

Изјава о истоветности штампане и електронске верзије докторског рада

Име и презиме аутора Ahmed Algellai_____

Број индекса _____

Студијски програм инжењерство материјала_____

Наслов рада „Adheziona svojstva fotopolimerizujućih kompozitnih filmova na bazi metakrilata i čestica aluminijum oksida za primenu u stomatologiji", „Adhesion properties of UV-curing methacrylate - alumina particles composite films for use in dentistry"

Ментор Радмила Јанчић Хајнеман _____
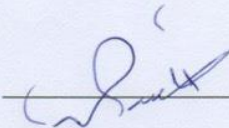
Потписани/а _____

Изјављујем да је штампана верзија мог докторског рада истоветна електронској верзији коју сам предао/ла за објављивање на порталу **Дигиталног репозиторијума Универзитета у Београду.**

Дозвољавам да се објаве моји лични подаци везани за добијање академског звања доктора наука, као што су име и презиме, година и место рођења и датум одбране рада.

Ови лични подаци могу се објавити на мрежним страницама дигиталне библиотеке, у електронском каталогу и у публикацијама Универзитета у Београду.

Потпис докторанда

У Београду, 25.06.2018_____

Прилог 3.

Изјава о коришћењу

Овлашћујем Универзитетску библиотеку „Светозар Марковић" да у Дигитални репозиторијум Универзитета у Београду унесе моју докторску дисертацију под насловом:

„Adheziona svojstva fotopolimerizujućih kompozitnih filmova na bazi metakrilata i čestica aluminijum oksida za primenu u stomatologiji", „Adhesion properties of UV-curing methacrylate - alumina particles composite films for use in dentistry"

која је моје ауторско дело.

Дисертацију са свим прилозима предао/ла сам у електронском формату погодном за трајно архивирање.
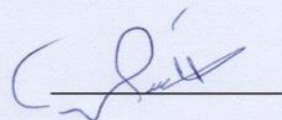
Моју докторску дисертацију похрањену у Дигитални репозиторијум Универзитета у Београду могу да користе сви који поштују одредбе садржане у одабраном типу лиценце Креативне заједнице (Creative Commons) за коју сам се одлучио/ла.

1. Ауторство

2. Ауторство - некомерцијално

3. Ауторство – некомерцијално – без прераде

4. Ауторство – некомерцијално – делити под истим условима

5. Ауторство – без прераде

6. Ауторство – делити под истим условима

(Молимо да заокружите само једну од шест понуђених лиценци, кратак опис лиценци дат је на полеђини листа).

Потпис докторанда

У Београду, 25.06.2018_____

CV of the candidate

Ahmed A. Algellai was born on 23th february 1971 in Misurata, Libya. The primary and secndary school as well as the College of medical Technology he compleated in Misurata Libya. The candidate compleated master studies at College of medical Technology at the department of Public Health department of Dental Technology in 2007.

At the department of Materials Science and Engineering he enroled in doctoral studies in 2013 and he compleated all exams according to the program.

In his home country he wroked at the College of medical Technology as engineer of medical technology at the university from 1998 to 2006. From 2011 he is the Director of the Society for Dental Service that is a volontary society for dental service in Misurata.

Biografija kandidata

Kandidat Ahmed A. Algellai rođen je 23.02.1971. godine u Misurati, Libija. Osnovnu i srednju školu, kao i fakultet College of medical Technology završio je u Misurati, Libija. Master studije na odseku za javno zdravlje završio je 2007 godine na College of medical Technology, Misurata na profilu Dentalne tehnologije završio je 2007. godine.

Na Katedri za konstrukcione i specijalne materijale na Tehnološko-metalurškom fakultetu Univerziteta u Beogradu upisao je doktorske studije 2013. godine i sve ispite po nastavnom planu i programu položio.

Nakon završetka osnovnih studija, radio je na Univerzitetu u nastavi iz dentalne tehnologije kao inženjer medicinske tehnologije u periodu 1998-2006. na Koledžu za medicinsku tehnologiju u Misurati u Libiji. Od 1997 do 2009 radio je u Libijskom komitetu u Misurati. Od 2011 je direktor Dobrotvornog društva za pružanje stomatoloških usluga.